DEVELOPMENT OF AN ASYNCHRONOUS SOLAR-POWERED COOKER

by

P. Femi Akinwale

Submitted to the Department of Mechanical Engineering
in Partial Fulfillment of the Requirements
for the Degree of Master of Science in Mechanical Engineering

at the

Massachusetts Institute of Technology

June 2006

Signature of Author ……

Department of Mechanical Engineering

June 5, 2006

Certified by……..

David Gordon Wilson

Professor Emeritus of Mechanical Engineering

Thesis Supervisor

Accepted by…….

Lallit Anand

Professor of Mechanical Engineering

Chairman, Department Committee on Graduate Students

DEVELOPMENT OF AN ASYNCHRONOUS

SOLAR-POWERED COOKER

by

P. Femi Akinwale

Submitted to the Department of Mechanical Engineering
on 5 June 2006
in partial fulfillment of the requirements for the
Degree of Master of Science in Mechanical Engineering

ABSTRACT

One reason that solar cookers have not gained widespread acceptance is because their use has proved inconvenient and impractical. Users are restricted to cooking when, and where, the sun is shining. Furthermore, the cooking temperature can not readily be raised or lowered as desired.

In contrast, the Wilson solar cooker is designed to permit use under conditions characterized by low or no insolation. Furthermore, the design would facilitate users adjusting temperatures. These temperatures would reach levels as high as 258 ^{0}C. In order to validate the concept, construction of one prototype was initiated.

Lithium nitrate, the heat-storage material, was shown to meet the stated requirements of storing heat at a constant temperature of 258 ^{0}C for up to six hours. Furthermore, this heat-storage material stored heat at temperatures above the boiling point of water, for up to 25 hours. Thus, it is expected that a meal for six people can be prepared up to six hours after charging of the thermal battery.

Thesis Supervisor: Professor David Gordon Wilson

Title: Professor of Mechanical Engineering

TABLE OF CONTENTS

TABLE OF CONTENTS

TABLE OF CONTENTS

LIST OF TABLES

Number

LIST OF FIGURES

Number Page

LIST OF FIGURES

LIST OF EQUATIONS

NOMENCLATURE

A) Symbols

A	=	area	m^2
c	=	specific-heat capacity at constant pressure	J/(kg.K)
Δ	=	difference	
E	=	thermal energy	J
h_f	=	latent-heat capacity	J/kg
I	=	solar irradiance	W/m^2
m	=	mass of material	kg
k	=	thermal conductivity	W/mK
ρ	=	density	kg/m^3
η	=	efficiency	
r	=	radius	m
SA	=	surface area	m^2
t	=	time	s
T	=	temperature	^0C
V	=	volume	m^3
x	=	distance	m

B) Subscripts

amb	=	ambient
des	=	desired
cool	=	cooling
f	=	fusion
i	=	inner
o	=	outer
pipe	=	cylindrical surface of pipe
tb	=	thermal battery
top	=	top surface of sealed pipe
scc	=	solar concentrating collector
sun		(self-explanatory)

ACKNOWLEDGMENTS

The author wishes to thank all her family members for their unwavering support. In addition, she is immensely grateful to Professor Wilson, for his guidance and mentorship throughout the duration of the project. In addition, Jakob Hopping deserves many thanks for his assistance, insight, and friendship.

Lastly, the MIT Electronic Research Society (MITERS) was particularly generous with supplies and equipment, in support of this research project.

GLOSSARY

Absorber. A device that converts light energy to thermal energy.

Absorptance ratio. Ratio of absorbed solar radiation flux to the incident radiation flux.

AWS. American Welding Society.

Collector. Device used to capture solar radiation .

Concentration ratio. Ratio of the cross-sectional area of the incoming radiation to the cross-sectional area of the radiation after concentration.

Concentrator. Device used to raise the temperature of incoming radiation, by focusing incoming irradiation onto a reduced area.

Emissivity. Ratio of the emissive power of a surface to the emissive power of a black surface at the same temperature.

Emitter. A body that radiates thermal energy.

Latent heat. Thermal energy stored or released as a material changes phase (solid/liquid or liquid/gas) at constant temperature and pressure.

Latent heat capacity. Thermal energy stored or released per unit mass of material undergoing a phase change.

ME. Mechanical engineering.

MIT. Massachusetts Institute of Technology.

MSDS. Material safety data sheet. It contains information on possible chemical hazards and safe use of a material.

Phase-change material (PCM). A substance used for energy storage because of its change of state, which occurs at a fixed temperature. Phase-change materials usually have large latent-heat capacities.

Reflection. Change in direction of a wave front at an interface between two dissimilar media so that the wave front returns into the medium from which it originated.

Sensible heat: Thermal energy stored or released as a material changes temperature.

Specific heat capacity. Thermal energy stored or released by a unit mass ot material per unit of temperature.

Solar Cooker. Device that is powered by solar radiation. It is used to supply heat for preparing meals.

Tracking. The mechanism whereby a device follows the apparent movement of the sun.

GLOSSARY

Thermal battery. A device that stores thermal energy to be released for use later.

Transmission. Propagation of light waves through a medium.

VITA. Volunteers in Technical Assistance.

Chapter 1) Introduction

Solar cookers convert solar radiation into heat, which is used to cook food. Such cookers - in principle - require very low operating costs, because they rely on an energy source that is free, abundant, and renewable. In addition, their operation inflicts virtually no damage on the environment. Numerous designs (over 200) already exist. Many designs are described in books[1] and in the technical literature[2]. Even more are described on the internet[3]. A few are available commercially and even fewer enjoy widespread use.

This low level of acceptance is primarily because most solar cookers have one drawback. Cooking must occur when, and where, the sun is shining.

A) Mechanism of operation

Solar cookers rely on three physical processes:

i) Collection

The goal of collection is to direct solar rays towards an absorber surface. The process begins when solar rays fall on a collector. The average solar iradiation is a physical constant (1300 W/m^2)[4]. Therefore, as shown in Equation 1, the gross amount of energy collected is directly proportional to the surface area used for collection.

To maximize energy collection, rays must be perpendicular to the collector surface. This requires tracking along two axes. The first axis follows the apparent daily movement of the sun from east to west. The second axis follows the apparent yearly movement of the sun from a horizon angle of $L-23.45^o$ to $L+23.45^o$, where L is the local latitude. In Cambridge (Massachusetts), the latitude is 42^0, so the collector would oscillate yearly from 18.55^0 to 65.45^0.

The technique used for transferring the collected rays to the absorber is determined by the position of the absorber surface with respect to the collector. The two choices for that transfer are reflection and transmission.

For high-temperature applications, concentration is necessary. Such temperatures are facilitated by the reflection of solar rays from one surface onto a smaller area, so that the intensity of the light energy is increased.

The three major types of concentrators are[2]:

(a) stationary and seasonally adjusted;

(b) line concentrators; and

(c) point concentrators.
Concentration ratios range from 200 for two-dimensional collectors to 40,000 for three-dimensional collectors with tracking.

ii) Absorption

Once sunlight from the collector reaches the absorber, the light energy must be converted to heat. The ratio of radiated light energy to absorbed heat energy is the absorption efficiency. The two factors that govern this efficiency are the emittance ratio and the absorptance ratio. The value of both factors increase with the temperature of the absorber. Overall efficiency increases as the ratio of absorptance to emittance increases.

Two mechanisms can be used to increase the absorptance ratio.

(a) Fins

These trap solar rays by increasing the number of reflections each incident ray undergoes, before finally being absorbed.

(b) Selective coatings

These utilize the same principle as fins, but on a microscopic scale. Owing to ease of manufacture, selective coatings are used more widely than fins. Values of absorptance ratio and emissivity for various materials are shown in Table 1[4].

Table 1: Absorptance ratio and emissivity for selective coatings

NAME	Absorptance ratio	Emmissivity	Ratio
Black coatings			
Anodize Black	0.88	0.88	1
Carbon Black Paint NS7	0.96	0.88	1.09
3M Black Velvet Paint	0.97	0.91	1.07
Polyethylene Black Plastic	0.93	0.92	1.01
CONDUCTIVE PAINT			
Brilliant Aluminum Paint	0.3	0.31	0.97
Epoxy Aluminum Paint	0.77	0.81	0.95
ANODIZED ALUMINUM SAMPLES			
Black	0.65	0.82	0.79
Blue	0.53	0.82	0.65
Brown	0.73	0.86	0.85
METALS AND CONVERSION COATINGS			
Black Chrome	0.96	0.62	1.55
Buffed Aluminum	0.16	0.03	5.33
Inconel X Foil (1 mil)	0.52	0.1	5.2
Stainless Steel Polished	0.42	0.11	3.82
VAPOR DEPOSITED COATINGS			
Aluminum	0.08	0.02	4
TAPES			
4253M Aluminum Foil	0.2	0.03	6.67
Y93603M Aluminzed Mylar	0.19	0.03	6.33

As shown in Table 1, materials with dark colors (black chrome and black paint) have the highest absorptance ratio. Such materials (with high absorptance ratios and high absoptance:emmissivity ratios) are the most desirable for solar energy conversion applications.

iii)Heat transfer and storage

Various mechanisms exist to store heat and transmit it to the food, so that heat losses are minimized. The mechanism used is governed by the spatial and temporal position of the food in relation to the absorber.

The three major classes of heat-storage technologies are listed below.

(a) Sensible-heat storage.
Heat is stored by raising the temperature of a material. The amount of heat stored = $mc\Delta T$.

(b) Latent-heat storage.
Heat is stored by causing a change in phase - either from solid to liquid, or from liquid to solid. The amount of heat stored = mH_f.

(c) Thermochemical-reaction heat storage:
Most reactions either require energy absorption or involve the release of energy. Thus, heat can be stored or released by reversing the direction of the reactions.

In many cases, two or more of the major physical processes may be combined in one entity. For instance, in box cookers, the pot serves as the absorber and collector, eliminating the need for radiation transfer from collector to the absorber.

Generally, cooking takes place at the same time and in the same location as absorption and collection. By avoiding this restriction, the WSC offers virtually unprecedented convenience in the realm of solar cooking.

B) Goals

Prior to the inception of this project, two students[5,12] working under the supervision of Professor Wilson conducted analytical studies that led to recommendations for the construction of the WSC. However, the concept was not tested since no prototype had been built. This research project was embarked upon in order to validate the feasibility of the WSC, by building one prototype and testing it. The following objectives were outlined.

i) Deliverables

On a warm, sunny, and dry day in Cambridge, Massachusetts - the WSC prototype would collect sufficient heat so that even after four hours from the completion of solar collection, it would still heat 1kg of water at room temperature to boiling point within 15 minutes. Once the boiling point is attained, it would maintain that temperature for one hour.

The purpose of this project was to investigate of the practicability of the WSC. Therefore, owing to time constraints – some desirable features would have to be omitted – if they did not significantly impede basic functionality. If successful, thermal storage would be the most significant advantage this cooker enjoys, in comparison with other solar cookers. Thermal storage was therefore earmarked to receive the most attention.

ii) Planned features

(a) Total weight less than 80 pounds.

(b) Cost less than $50 US.

(c) Ease of manufacture in non-industrialized countries.

iii)Deferred features

(a) Salt-state indicator – a mechanism that warns that charging is complete.

(b) Operator control of stovetop heat-transfer rate during cooking.

(c) Automatic tracking of the sun's apparent movement.

C) Key Topics

Te following variables were of greatest importance in measuring the performance of the Wilson solar cooker. Hence, experiments were designed to elicit the factors that control the following parameters.

i) Heat-absorption rate during charging

The rate of net heat absorption by the cooker during thermal charging.

ii) Heat-loss rate during storage

The rate of heat loss during storage as a function of storage time and number of modules stored.

iii)Heat-transfer rate during cooking

Rate and efficiency of thermal energy transfer from thermal battery to pot during cooking.

iv) Useful heat

The proportion of heat stored that can be transferred to a cooking pot.

v) Maximum system temperature

The highest temperature that the system can attain without negative effects.

First, the context for solar cookers is detailed in the background chapter. In the next chapter, the methods used to design, build, and test the first WSC prototype are discussed. Subsequently the observations made are presented in the results and discussion chapter. Lastly, those findings are incorporated into recommendations for future design work.

Chapter 2) Background

A) History

Solar cookers have been in existence for centuries. The first patent is dated 1894[6]. Even though there are more than two hundred functional designs, the cookers have not gained widespread acceptance. This is surprising, because they offer many advantages. Firstly, they rely on a virtually infinite energy source. Secondly, the user usually does not have to pay to utilize the energy source. Thirdly, he does not have to travel far to gain access to sunlight. It streams into his residence on normal days. Fourthly, the use of the devices does not degrade the environment.

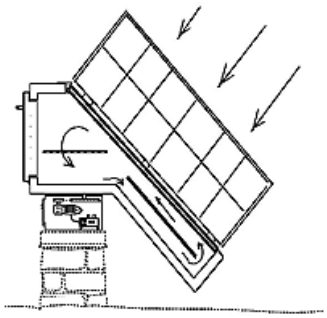

Figure 1: Tracking box cooker

All of this is in contrast to the difficulty faced as part of the process of obtaining cooking equipment and supplies, in industrializing countries. Firstly, low levels of income create challenges in purchasing cookers. Secondly, traditional energy supplies are scarce, regardless of whether they are in the form of petroleum by-products, coal, wood, or electricity. Lastly, the use of the above-mentioned energy sources does have an unfavorable impact on the environment.

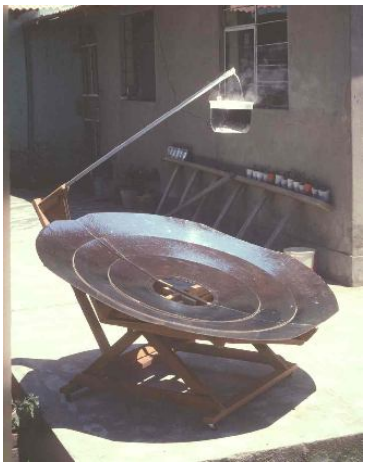

Figure 2: Fresnel solar cooker

Incidentally, places that fit this description, for example sub-Saharan Africa and Southeast Asia, tend to enjoy high levels of solar insolation. Therefore, many of the listed problems could be alleviated by solar cookers.

Why are solar cookers not being used more widely? Is it because they do not work? Are they difficult to use? Do people dislike them? Might potential users be unaware of their existence? Alternatively, are they too difficult to obtain? Perhaps they are too expensive.

Figure 3: VITA solar cooker[7]

i) Temporal restrictions

From examining Figure 2 and Figure 3, it appears the answer leans most heavily toward the third option, because the user is restricted to preparation of the food when the sun is shining. Furthermore, the cooking must be done in an extremely unnatural fashion. Many solar cookers call for suspending pots at the focal point of a reflector, or for placing the pots in enclosures, as shown for the tracking box cooker in Figure 1. Monitoring of cooking and addition of ingredients become more challenging with the pot inside an enclosure.

Figure 4: Parabolic solar cooker

Others require lengthy cooking times due to the relatively low operating temperatures. All of these stipulations combined, place a cumbersome burden on the user, one that is rejected very frequently.

Some parabolic solar cookers do attain relatively high temperatures. The specifications for the parabolic solar cooker in Figure 4 predict a power output of 500 watts, which can bring one liter of water to boil in less than thirty minutes.

Figure 5: Clear Dome solar cooker

The highest temperatures reported for solar-powered cookers is by Clear Dome solar, with some products attaining 1371 ^{0}C.

Since many families have hot meals for breakfast and dinner, the following question arises from reviewing the five solar cookers mentioned above. How is food to be prepared in the morning or at night, when there is no sun light? What about overcast days? Apparently, users would need to have an alternative means of cooking. Those with low incomes – the target audience, do not easily meet this requirement for the possession of multiple cookers.

ii) Spatial restrictions

A secondary reason for the low level of acceptance is that solar cookers generally require cooking outdoors. For many potential users, this is not easy to do. Consider the case of apartment dwellers. Most share outdoor space with other apartment residents. In this and many other situations, operation of a solar cooker would require sacrificing privacy.

Another problem with the requirement of cooking outdoors is inclement weather. To utilize a conventional solar cooker on rainy or cold days, the user will likely be subjected to physical discomfort.

12 years ago, Professor David Gordon Wilson (of the MIT mechanical engineering department) designed a solar cooker that eliminates these requirements – by converting absorbed radiant energy to stored thermal energy for later use, possibly at a different location. The Wilson solar cooker (WSC) can therefore be used at the convenience of the user, under conditions of low or no insolation, for example – a kitchen inside a building at night.

Similar cookers, that store energy for later use, have been developed in the last four years. In one study, acetanilide was used in a three-reflector solar cooker, with temperatures in the range of 110 to 120 ^{0}C[8]. The same authors also used erythritol with an evacuated tube solar collector. The reported operating temperatures were similar[9]. In a third study, Murty and Kaanthed[10] propose the novel concept of utilizing the phase-change material (transparent lauric acid) as insulation. Reported temperatures were very low (42 ^{0}C). Another application was developed at the University of Salta, in Argentina. Solar heated aluminum bars at 204 ^{0}C, after transfer to an oven, were used to prepare food for up to forty people.

Figure 6: Stored-heat concentrating reflector in Salta, Argentina

iii)Temperature restrictions

The drawbacks to the last four systems combine to form the third reason for the low level of acceptance of solar cookers. The drawbacks involve low temperatures, fixed temperatures or both. A modern electric or gas cooker can boil one kg of water in five minutes. This is certainly not the case with most solar cookers to date. To the contrary, they operate at temperatures less than 120 ^{0}C. Therefore, they typically require up to 180 minutes[7] to bring 0.15 kg of water to boiling and 420 minutes[8] to bring 10 kg of water to boiling. This slows cooking time considerably - rendering it very unattractive to anyone who does not have the time or willingness to wait two hours for a meal. This rules out many people.

In response, to increase cooking speed, the Wilson solar cooker is designed to operate at temperatures up to 250^{0}C with provisions for the user to adjust the temperature as desired.

B) Components

Consequently, Professor Wilson[11] proposed the following solar cooker design in order to address the issues raised above. Those issues are addressed by designing the cooker to store absorbed solar energy for later use.

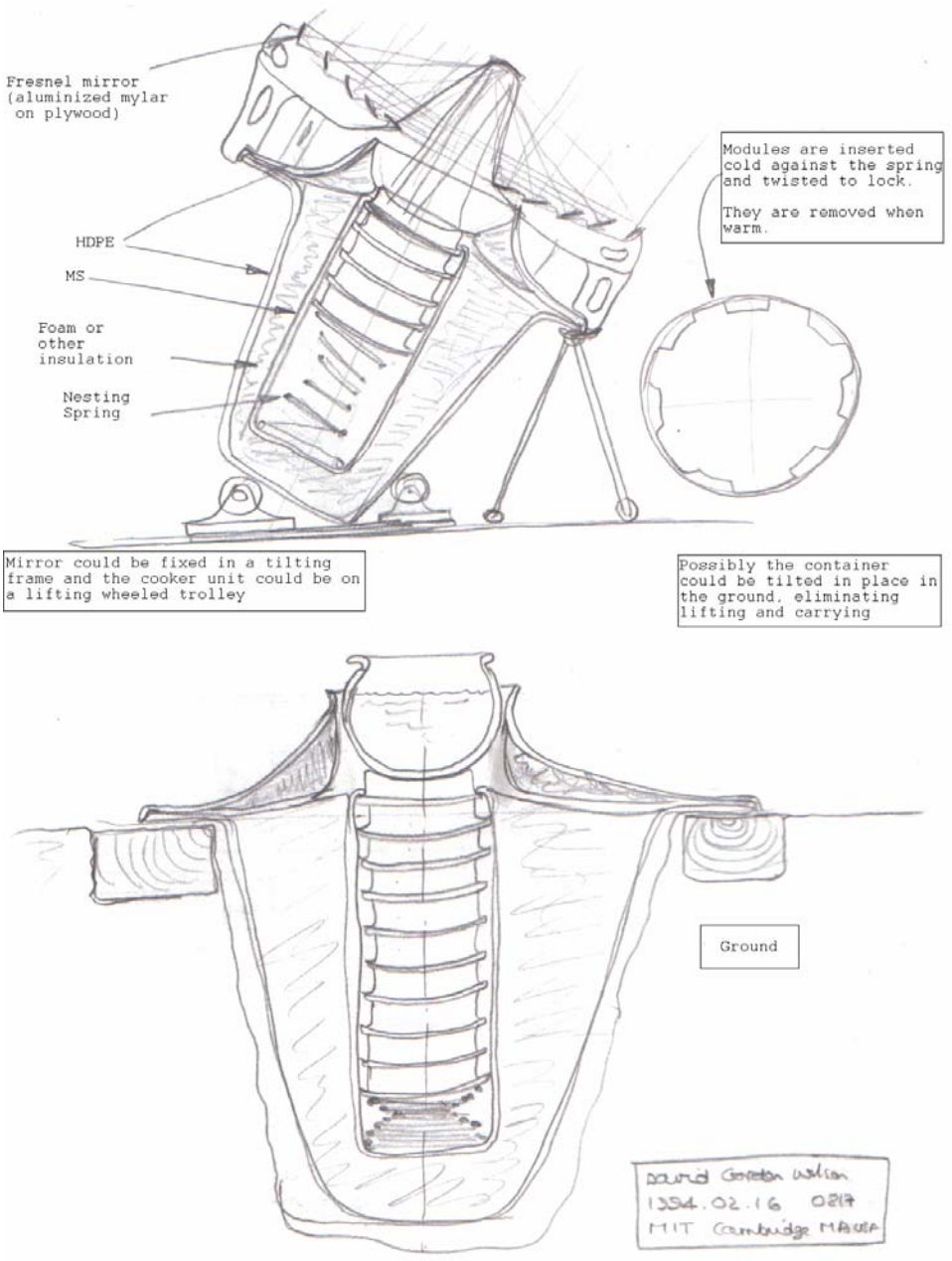

Figure 7: Early Wilson solar cooker design

The proposed design specifies three primary components- a collector, a thermal battery, and a stovetop.

i) Collector

The collector is made up of two reflectors. The primary reflector is a Fresnel mirror constructed in accordance with instructions provided for the VITA solar cooker. The secondary reflector is suspended at the focal point of the primary reflector. An aperture in the Fresnel mirror permits transmission of the reflected rays to the absorber beneath.

ii) Thermal battery

The thermal battery consists of the insulated storage container and the storage modules.

(a) Storage modules

Each storage module consists of two metal plates welded together and filled with the heat-storage material. The storage modules operate in two modes.

1. Absorber function. Charging phase.

Charging would normally occur during periods of high insolation. The top surface of the highest module serves as the absorber, accepting radiation reflected from the secondary mirror. To enhance conversion of solar radiation to heat, the absorption surface should therefore be:

colored black;

finned; and/or

coated with a highly absorptive material.

As this heat is conducted to adjoining modules, the temperature of the enclosed storage material rises. If a phase-change material is used, the modules store sensible heat until the melting point is reached, at which point energy is stored as latent heat. Once all of the salt is melted, any further heat absorbed is again stored in the form of sensible heat as the molten salt's temperature rises beyond its melting point. The modules would be removed when fully charged, to a separate enclosure optimized for storage and possibly, cooking.

2. Stovetop function. Discharging Phase.

When the collector and aperture cover are removed, a cooking pot can be placed above the modules. At this point, cooking commences.

(b) Insulated storage container

The insulated storage container houses the modules. Its primary purpose is to prevent heat loss from the modules during charging as well as during the time interval between charging and cooking. The container consists of an inner and outer cylindrical casing, separated from each other by an insulating material, such as foam. The opening at the top of the container may be sealed, with an aperture cover, to reduce thermal losses. For this, a transparent material (glass or plastic sheets) would be used, to permit reception of solar radiation from the secondary reflector.

iii)Stovetop

When the collector is removed, a cooking pot can be placed directly atop the highest module, at which point cooking commences.

C) Analysis

Two of Professor Wilson's previous students, Benjamin Matteo[5] and Chimba Mkandawire[12], analyzed the above design. As described in the next section, they derived pertinent operating conditions and design values for the WSC.

i) Collection.

The factors that influence the energy collected are listed below.

(a) The concentration ratio

Higher concentration ratios reduce the absorber area required to absorb a given quantity of radiant energy.

(b) Heat losses.

Four mechanisms exist for heat loss.

1. Reflection
   Energy lost between incidence and reflection.

2. Transmission
   Energy lost between transmission from the collector to the absorber.

3. Absorption
   As shown in Table 1, most paints (like black chrome)[4] have an absorptance/emissivity ratio of one. This requires a concentration ratio of 80 to achieve temperatures of 650K. In the process of energy conversion from light to heat, some energy is lost.

4. Leakage
   Energy lost from the system due to conduction and convection.

ii) Thermal charging

The time needed to collect a give amount of thermal energy is given by:

$$t_{heat} = \frac{\Delta E_{tb}}{\eta_{scc} I_{sun} A_{scc}}$$

Equation 1: Module charging time

The following estimated values are used to calculate the time needed to collect a given amount of thermal energy. The results are shown in Table 2.

(a) A solar collector efficiency of 50 %.

(b) An average solar irradiance of 1300 W/m^2.

(c) A thermal energy requirement for each meal of 12.7 MJ.
This value is estimated by calculating the energy required to:
raise the equivalent of six liters of water from room temperature to boiling; and
maintain the boiling point temperature for one hour.

Table 2: Module charging time at 50% collection efficiency, with tracking

Collector Radius (m)	Time (h)
1	0.84
0.75	1.49
0.5	3.37

Without E-W tracking, energy yield is up to 0.85% of that with full tracking.

iii)Thermal dissipation

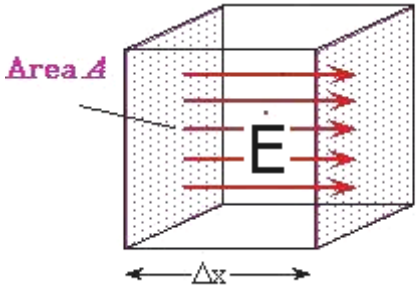

Figure 8: Thermal conduction model

For the infinitesimal mass shown in Figure 8, the conductive heat-transfer rate is given by:

$$\frac{dE}{dt} = kA\frac{dT}{dx}$$

Equation 2: Rate of thermal energy transfer

From equation 2, the time required for this energy to be dissipated is:

$$t_{cool} = \frac{\Delta E}{kA}\left(\frac{dT}{dx}\right)^{-1}$$

Equation 3: Time required for thermal energy dissipation

The total thermal energy loss from the thermal battery was estimated using a pipe insulation model, as depicted in Figure 9

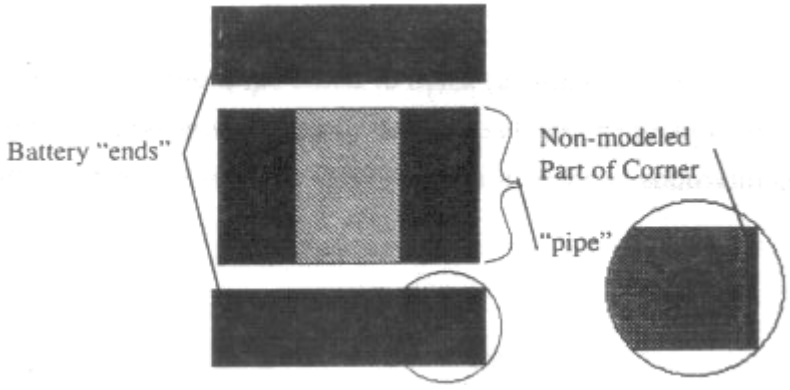

Figure 9: Pipe insulation model

Integrating Equation 2 over the surface of the pipe gives

$$\frac{\dot{E}_{pipe}}{SA_{pipe}} = \frac{\Delta T}{\frac{r_o}{k}\ln\frac{r_o}{r_i}}$$

Equation 4: Heat loss through a cylindrical surface

Summing up heat losses from the top, bottom, and vertical surface gives

the overall heat-loss rate = $\left(1+2\frac{SA_{top}}{SA_{pipe}}\right)\dot{E}_{pipe}$

Equation 5: Total rate of heat loss through pipe insulation

iv) Module geometry design

The energy stored by the module is related to the temperature by the following equation:

$$\Delta E_{tb} = \rho_{LiNO_3} V_{LiNO_3}(c_{tb}\Delta T + \Delta H_f)$$

Equation 6: Module energy storage

ΔT is given by

$\Delta T = T_{desired} - T_{ambient}$

Equation 7: Module temperature difference

v) Spring design

Dividing the total module weight by the solid height of the spring gives the required spring constant.

Table 3: Spring geometry

Solid Height of Spring	1 in
Spring Constant	2850 N/m

D) Design

Upon completion of the analytical studies described above, Benjamin Matteo and Chimba Mkandawire recommended the two designs shown in Figure 10 and Figure 11.

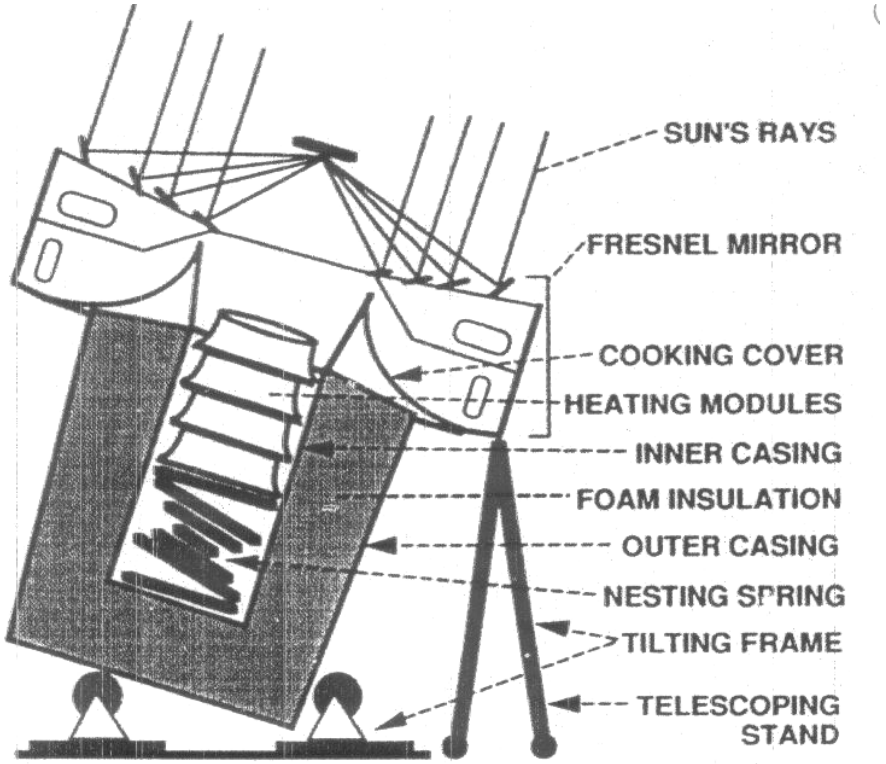

Figure 10: Recommended Wilson Solar Cooker: Version 1

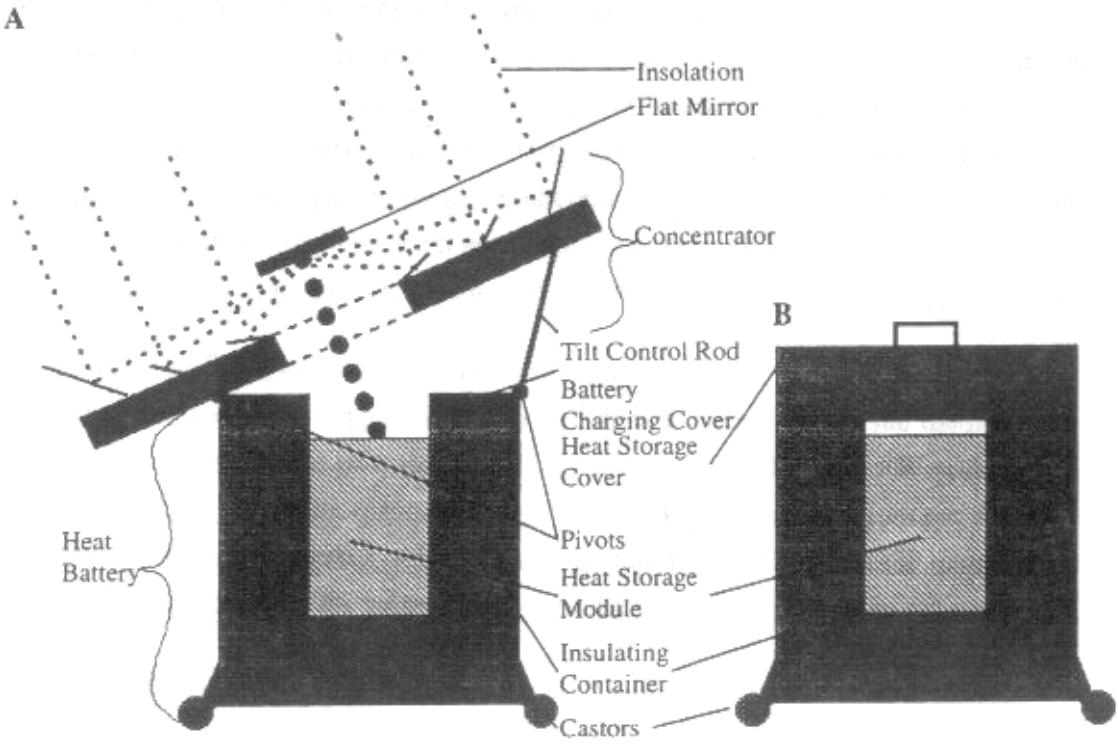

Figure 11: Recommended Wilson Solar Cooker: Version 2

Chapter 3) Methods

Given the advances in materials development during the ten years since the above designs were proposed, it seemed necessary to revisit some of those recommendations before construction commenced. Figure 12 shows the WSC design proposed for this project.

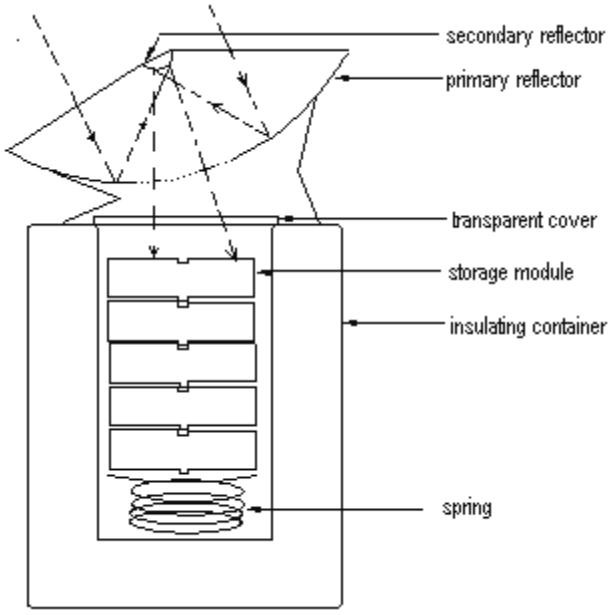

Figure 12: Proposed Wilson solar cooker design

First, a material was selected to act as the heat-storage material. Next, a metal was selected for the module container. Thirdly, the shape of the module container was designed. Fourthly, the module assembly was developed. Simultaneously, the insulating container was designed and developed by Jakob Hopping, an undergraduate student. Lastly, tests were formulated and executed.

A) Material selection

i) Heat-storage-material selection

(a) Heat-storage-material selection criteria.

The target users for the WSC were defined to be middle-aged women in rural areas of aggressively industrializing countries, such as Malaysia. Ideally, these users would have daily access to a space receiving solar insolation.

In addition, users would have someone to operate the device during absorption. This could prove time-consuming (up to six hours per day).

Accordingly, a heat-storage material was sought that exhibited the following characteristics, listed in order of precedence.

1. Safety

There was a strong possibility that selected laboratory chemicals might be introduced into the kitchens of people who are not necessarily familiar with such substances. Therefore, mechanisms were sought to prevent those users from coming into bodily contact with, or become unduly exposed to, chemical hazards.

In particular, the nitrate salts are known to pose specific safety risks. The nitrates of potassium and sodium are commonly used as explosives. The material safety data sheet (MSDS[13]) for the nitrates of potassium, sodium, and lithium specify the risk of explosions upon exposure to shock or heat.

2. Low cost

Regardless of how well the product is designed, it serves no purpose if the users can not afford it. Since the intended users are likely to earn relatively low incomes, and since the heat-storage material would likely be the largest component of the system, low cost was sought for the heat-storage material.

3. Readily available in developing countries

Importation of the heat-storage material would almost certainly increase the price of the WSC. Furthermore, local availability of the heat-storage material would encourage local manufacture, which would in turn enhance the local economy, which would then increase the buying power of the target users. The goal is to help people in underprivileged countries by stimulating their economy. Manufacturing the device in industrialized countries would only increase dependence on foreign economies.

4. Low density

Minimization of the total weight of the WSC was a design goal. Since the latent-heat energy stored is directly proportional to the mass of heat-storage material, it was important to find a heat-storage material with the lowest density possible.

5. High latent-heat capacity

In order to reduce both weight and volume, materials with the highest specific-heat capacity were sought.

6. High thermal conductivity

Once absorbed, thermal energy must be transferred quickly to the heat-storage material. Any delays in absorption would increase dissipation, directly reducing efficiency of heat storage.

7. Melting point above 250 ^{o}C

Operating temperatures above 250 ^{0}C were needed for three reasons:

a to enable reasonable cooking speeds;

b to permit baking; and

c to permit frying.

Therefore, the melting point of the heat-storage material must also exceed that temperature (250^{0}C).

(b) Heat-storage-material candidates.

The following materials were considered.

1. Sensible-heat-storage media

These materials would fulfill the first three requirements. However, unlike phase-change materials, the discharge temperature can not be kept constant.

Table 4: Required volume and mass for selected sensible heat media

Material	Heat capacity (J/kg-K)	Density (kg/m^3)	Required volume (cm^3)	Required mass (kg)	Material cost ($)
Ceramics:					
alumina	1,045	3,980	7,637	30.40	28.88
clay	937	1,009	33,586	33.90	
graphite	1,632	2,251	8,650	19.50	
Cerium dioxide (CeO_2)	171,069	7,280	26	0.20	3.76
Molybdenum disilicide ($MoSi_2$)	41,840	6,250	122	0.80	
Zirconium diboride ($ZrBr_2$)	289,616	18	0.10		7.88
Non-ceramics					
Concrete:	916	2,307	15,029	34.70	

Furthermore, sensible-heat-storage media have low thermal conductivity. Therefore, their use was removed from further consideration.

2. Phase-change materials such as the nitrate salts, tin, and proprietary compounds. Eutectic mixtures of sodium nitrate and potassium nitrate were likely candidates because they melt at desirable temperatures (such as 220 ^{0}C) and had been used previously to store thermal energy in solar applications.

Table 5: Thermal properties of nitrate phase-change materials

Material	Melting point (^{0}C)	Boiling point (^{0}C)	Density (g/cm^3)	Conductivity (W/mK)	Specific heat capacity (J/kgK)	Heat of fusion (kJ/kg)
Potassium nitrate	333	400	2.1	0.5	267	118
Sodium nitrate	308	308	2.26	0.5	200	185
Lithium nitrate	250		2.38		385	367

Lithium nitrate emerged as the top candidate because it possessed a high melting point (between 250 ^{0}C and 258 ^{0}C) as well as a high latent-heat capacity - twice that of potassium and sodium nitrate.

Table 6: Thermal properties of lithium nitrate

Melting point	623	K
Heat of fusion	367	kJ/kg
Specific-heat capacity	385	J/kgK
Conductivity	0.5	W/mK
Vapor pressure	unknown	

In spite of these favorable characteristics, lithium nitrate posed a safety risk since its material safety and data sheet predicted that it would explode when exposed to heat, shock or strong reducing agents. Measured values of the vapor pressure, as a function of temperature, are not available.

Table 7: Physical properties of solid lithium nitrate

Density	2.16 g/cm^3
Volume/kg.	0.46 l/kg
Weight required for the WSC to store 13 MJ	35.7 Kg / 78.6 lbs
Volume required for the WSC to store 13 MJ	15 l

In addition, the cost and availability of lithium nitrate were unfavorable. Lithium nitrate is sold at the rate of $9/lb and is not available in most developing countries. It is available in South Africa.

Table 8: Physical properties of liquid lithium nitrate

Density	1.78	g/cm^3
Specific volume	0.56	l/kg
Expansion ratio	21.4%	

ii) Module-material selection

(a) Module-material selection criteria

In addition to the heat- storage material, a module-material had to be chosen. The requirements were as follows.

1. Compatibility with the heat-storage material

   Any reaction between the heat-storage material and module-material could lead to explosion or degradation of either material. It could also lead to the production of undesirable products. Repeated temperature cycling could not be permitted to cause degradation of either heat-storage material or module-material.

2. Low density

   Reduction of the module-material's density would lead to a proportional reduction in weight.

3. Low cost

   Reduction in module cost was essential to satisfying the targeted total cost of $50 (US).

4. Available in developing countries

   This enables local manufacture for intended users.

(b) Module-material candidates. The following materials were considered.

Table 9: Properties of module-material candidates[14]

	Steel	Cast iron	Mild steel	Aluminum
Density (g/cm3)	7.9g/, 0.285 lbs/in^3	7.8	7.872	2.7
Coefficient of thermal expansion, linear 20°C	16.6 µm/m-°C			
Coefficient of thermal expansion, linear 500°C	19.8 µm/m-°C			
Specific heat capacity (J/kgK)	0.5	0.536	0.536	0.2241
Thermal conductivity (W/m-K)	16.3	80.4	50	167
Melting point (C)	1399 - 1421 °C			660

The three materials selected for testing were aluminum, mild steel, and stainless steel, since they are widely available.

1. Aluminum

Aluminum had the advantage of lightness, low cost and ease of manufacture. According to the MSDS, it posed the threat of reacting with lithium nitrate to create an explosion and form undesirable products.

2. Stainless steel

Stainless steel held the promise of reduced reactivity and corrosion. However, its density of 7.9 g/cm^3 is almost thrice that of aluminum (2.7 g/cm^3). Stainless steel also had the advantage of ease of joining (through welding or brazing).

Two grades of stainless steel were considered.

a 304 stainless steel

This steel has high resistance to elevated temperatures, oxidation, and corrosion. However it is difficult to machine. In view of the complexity of the proposed module design, machinability was a significant factor.

b 303 stainless steel

This steel is more expensive, but is easier to machine. However, its weldability is lower. The same factors that make this alloy corrosion resistant and strong also increase the difficulty associated with welding it.[15] This led to discarding it as a module-material candidate.

Figure 13: Relative machinability of steels[16]

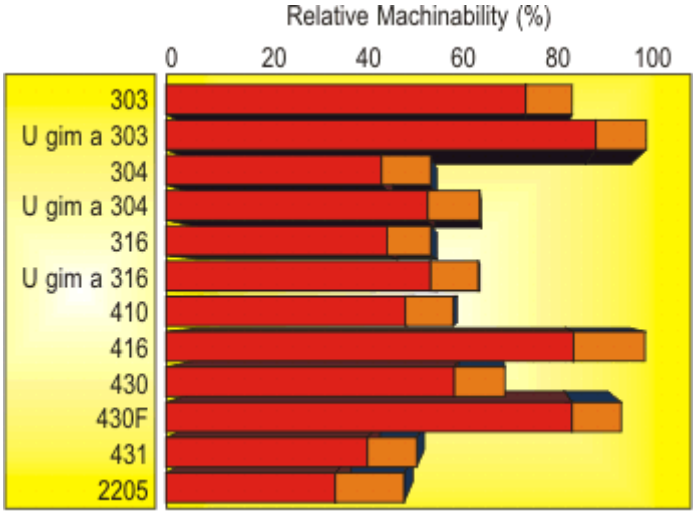

iii)Compatibility research

(a) Theoretical predictions for compatibility between $LiNO_3$ and common metals[17]

1. Pure lithium nitrate

The aluminum ion (Al^{3+}) has a higher position in the activity series than the lithium ion (Li^+). Therefore, aluminum should not displace the lithium ion (Li^+) in $LiNO_3$. Based on this, aluminum should not react with pure lithium nitrate.

2. Commercial grade lithium nitrate

However, commercial grade lithium nitrate commonly includes such impurities as Na, K, Ca, Al, Fe, CO_3, Cl, SO_4 and H_2O. These impurities accelerate the reactions between lithium nitrate and container metals. Therefore, the likelihood of corrosion is directly dependent on the concentration of these impurities. Thus, anhydrous $LiNO_3$ is reported as having high corrosivity for thermal storage applications. Use of nitrates with aluminum was not recommended for thermal storage.

3. Aqueous lithium nitrate

$LiNO_3$ inhibits corrosion of aluminum in aqueous alkaline solutions. This property is used in recycled nuclear waste to reduce corrosion of aluminum. However, this effect is reduced at high temperatures.

Also, mixtures containing $LiNO_3$ are used to anodize aluminum, which imparts resistance to corrosion.

(b) Theoretical predictions for $LiNO_3$ stability.

Reported decomposition temperatures are 258 ^{0}C (the melting point), 300 ^{0}C, and 327^{0}C. The decomposition products are lithium nitrite and oxygen. Decomposition can be reversed in oxygen at high temperatures.

Stability increases with mixtures of other nitrates. However, there are three disadvantages associated with these eutectic mixtures. Firstly, they melt at lower temperatures. Secondly, their heat of fusion is hard to find. Thirdly, nitrate eutectics eventually decompose with thermal cycling.

After searching the literature it was unclear whether lithium nitrate reacted with either stainless steel or aluminum, at temperatures below 350 ^{0}C. Two researchers were identified who had conducted experiments with nitrates.

The first was Dr. Robert Bradshaw[18] of the Sandia National Renewable Energy Laboratory. He had used the nitrates of potassium and sodium with stainless steel, at temperatures above 300 ^{0}C. He attested to the fact that no incidents had occurred and that he expected no problems with the planned experiments.

Another researcher, Dr. David Kerridge, at the University of Southampton in the United Kingdom[19] appeared to be the only one who had worked with lithium nitrate. His predictions were much different. He said that experiments with nitrates had proved to be very dangerous. In one case, a factory had exploded with many fatalities because an incompatibility had been introduced unknowingly. Owing to the safety concerns raised, aluminum was eliminated from further consideration.

iv) Compatibility tests

(a) Test 1: steel cup

This test was conducted to ascertain the compatibility of stainless steel with lithium nitrate. It was also conducted to investigate the effects of thermal cycling and the by-products of possible decomposition at high temperatures.

To test stainless steel, a stainless steel cup was selected measuring three inches in diameter and one inch in height. Its thickness was 0.050 in. To test mild steel, a mild steel cap was selected with a thickness of 0.5 inch. The cup was filled with lithium nitrate and sealed with the mild steel cap. The cap was tapered to ensure that no air, liquid or solid escaped. For three weeks, the cup was heated and cooled from 280 ^{0}C to 110 ^{0}C. Each cycle was repeated every thirty minutes. This provided 504 heating/cooling cycle repetitions. A Corning laboratory heater PC-420 was used to provide heat. A Grasslin digital timer switch was used for turning the heater on and off, every thirty minutes.

(b) Test 2: flat pouch

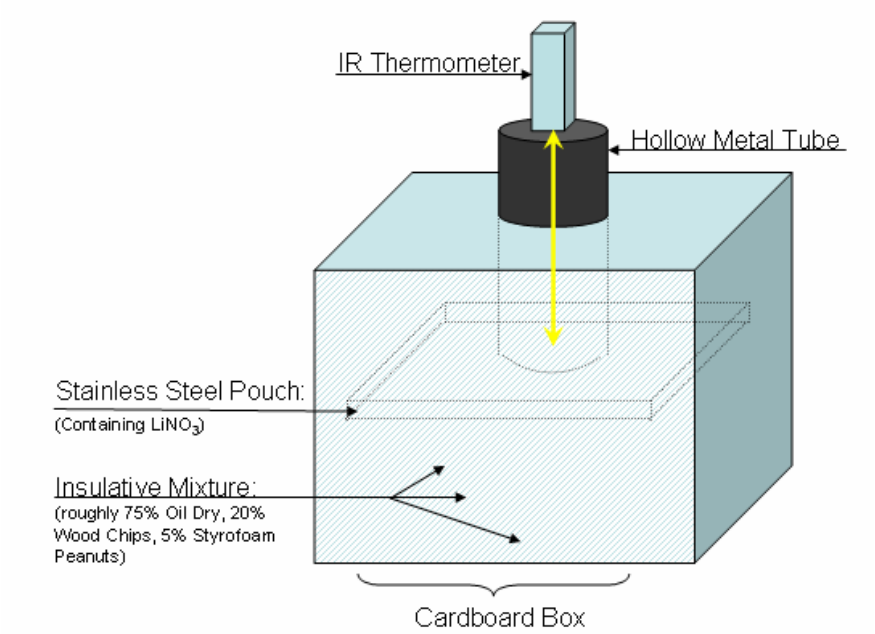

Figure 14: Flat steel pouch test set-up[20]

To address problems with leakage, brazing was identified as a joining method. In this test, carbon steel was tested for use as the module container material. Two square 4130 mild steel sheets (nine inches wide, nine inches long and 0.025 inches thick) were brazed together to form an envelope. This envelope was filled with one pound of lithium nitrate and heated from room temperature to 250 ^{0}C.

B) Module-shape design

The above-mentioned module-material tests had shown that there was no corrosion of either stainless steel after 504 cycles (equivalent to eighteen months of use). Doubts about corrosion of mild steel led to the initial choice of stainless steel as the module-material. Once material selection was completed, the shape of the module was designed.

i) Module-shape criteria.

In view of the requirements for the completed cooker, the shape of the module had to meet the following criteria.

(a) High surface area to volume ratio

The rate of conduction of thermal energy, from the module container to the heat-storage material, is directly proportional to the thermal conductivities of the module-body material and the heat-storage material. The thermal conductivity of lithium nitrate is low (0.5 W/mK). This is one-quarter the thermal conductivity of ice. This would lead to poor conduction to the heat-storage material.

To account for this, the area of the module container surface in contact with the heat-storage material was maximized by incorporating internal fins. Since conduction is proportional to surface area, this would facilitate a higher conduction rate.

(b) Minimum weight and volume

To conserve the total volume and weight of each module, it was necessary to optimize the amount of lithium nitrate enclosed in each module. In addition, there had to be enough room left for the lithium nitrate expansion that would accompany the increase in module temperature during charging.

(c) High absorption

The amount of heat stored by the module would be proportional to the amount of heat absorbed. In turn, the amount of heat absorbed by the module would increase with the area of the module used for absorption. Thus the module cross-sectional area used for absorption needed to be optimized.

Another approach to maximizing heat absorption was to increase the absorptance ratio by utilizing sprays, paints, gratings, and/or external fins.

(d) Portability

The module had to be designed in such a way that it was easy for the user to handle. The initial version of the cooker might require that the user manually removes fully heated modules and places them in a separate storage location. So each module had to be designed so that the user would be able to gain access to it, and easily carry it for more than 30 seconds at 300 ^{0}C. This would require weights as low as four lbs and handles which remained cool enough not to burn the user.

ii) Module-shape selection

Professor Wilson had originally proposed using two finned circular plates. The proposed design is shown below.

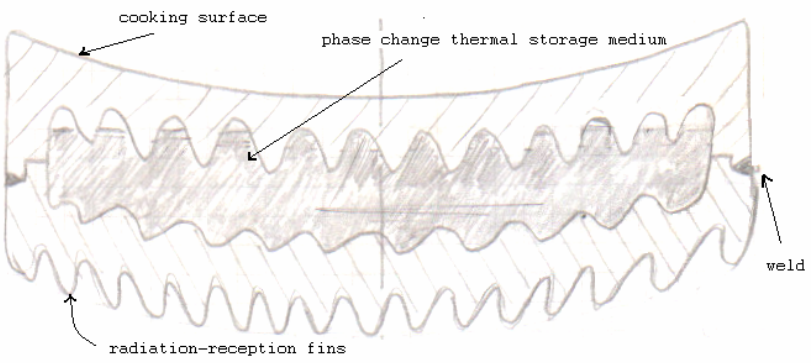

Figure 15: Early module design

This proposal was examined by two of his undergraduate students[5, 12]. They performed thermal modeling and analysis, which resulted in minor modification to his proposal. Their suggestions are shown below.

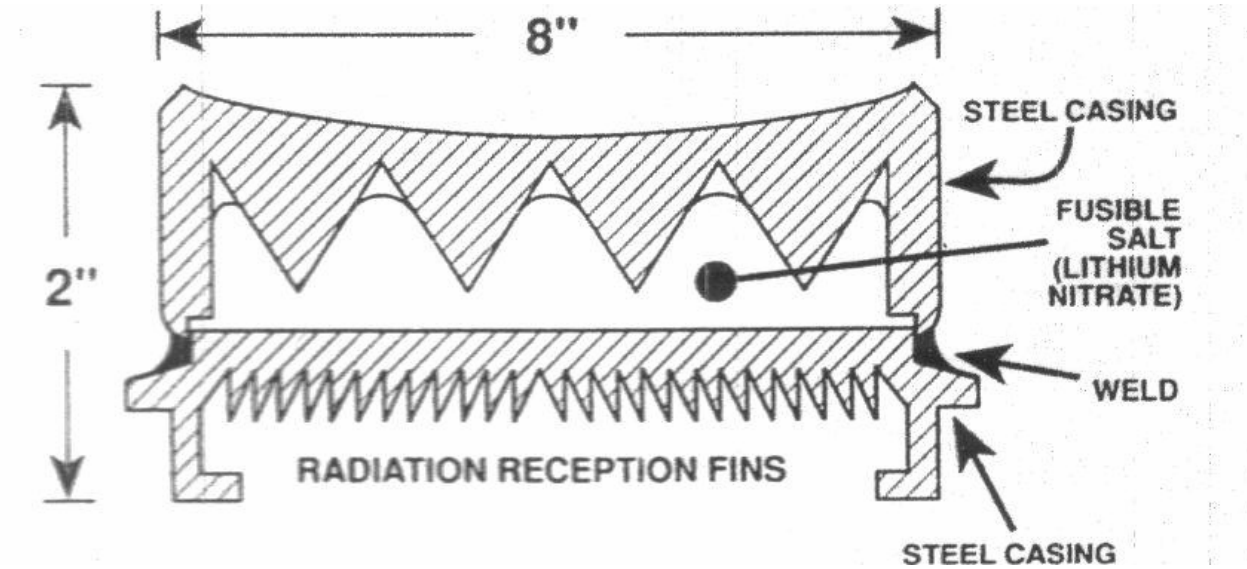

Figure 16: Revised module design

The original design and subsequent recommendations were used as the starting point for the module design. The first modification was the removal of the external fins associated with increased radiation absorption. In view of the complexity involved, incorporation of these fins was deferred for a later stage of the project.

The design of the module was then carried out by following the two steps listed.

(a) Optimization of the surface area to volume ratio.
ProEngineer was used for the drawings and modeling. The surface area to volume ratio for each design was computed. Subsequently, the module dimensions were revised in order to increase that ratio.

(b) Allowance of enough room for lithium nitrate expansion upon heating and liquefaction. The equation for lithium nitrate expansion[21] is listed below.

$$\rho(T) = \rho_m - \rho_T(T-T_m)$$

Equation 8: Lithium nitrate thermal expansion

The values for the constants in Equation 8 and the valid temperature range (T_{min}, T_{max}) are listed below.

Table 10: Lithium nitrate thermal expansion constants

ρ_m (g/cm^{3}K)	ρ_T (g/cm^{3}K)	T_m (^{0}C)	T_{min} (^{0}C)	T_{max} (^{0}C)
1.781	0.000546	253		441
1.93	0.000549	0	273	309

Thus, the expected expansion is up to 21%, as the module is heated from room temperature to 300 ^{0}C.

Figure 17 and Figure 18 show three-dimensional and two-dimensional views, respectively of the selected design.

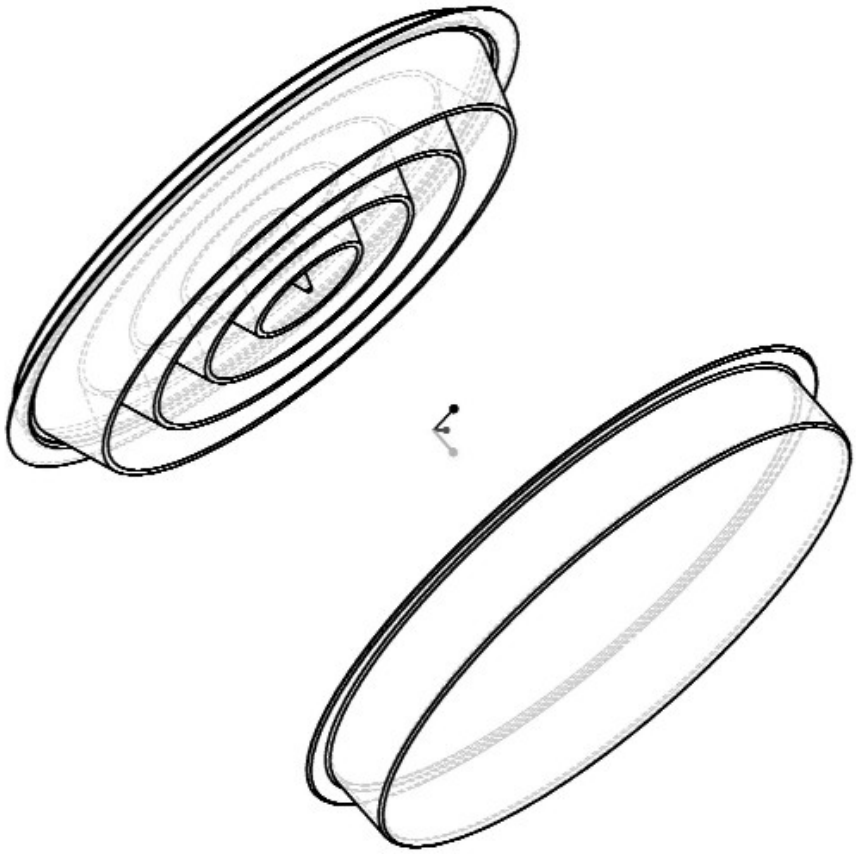

Figure 17: Three-dimensional view of the design selected for the module top and bottom

The required module design parameters for the specified heating load of 13 MJ, are given below.

Table 11: Module geometry design values (at room temperature)

Density of Steel	7.9	g/cm3
Density of solid Lithium nitrate	2.38	g/cm3
Single module		
Diameter	15	in
Thickness (external height)	1	in
Weight of salt	4.1	kg
Volume of salt	1.9	l
Volume of steel	0.67	l
Volume of air space	0.23	l
Total volume	2.8	l
System		
Number of modules required	8	
Volume	23.2	l
Height	8	in

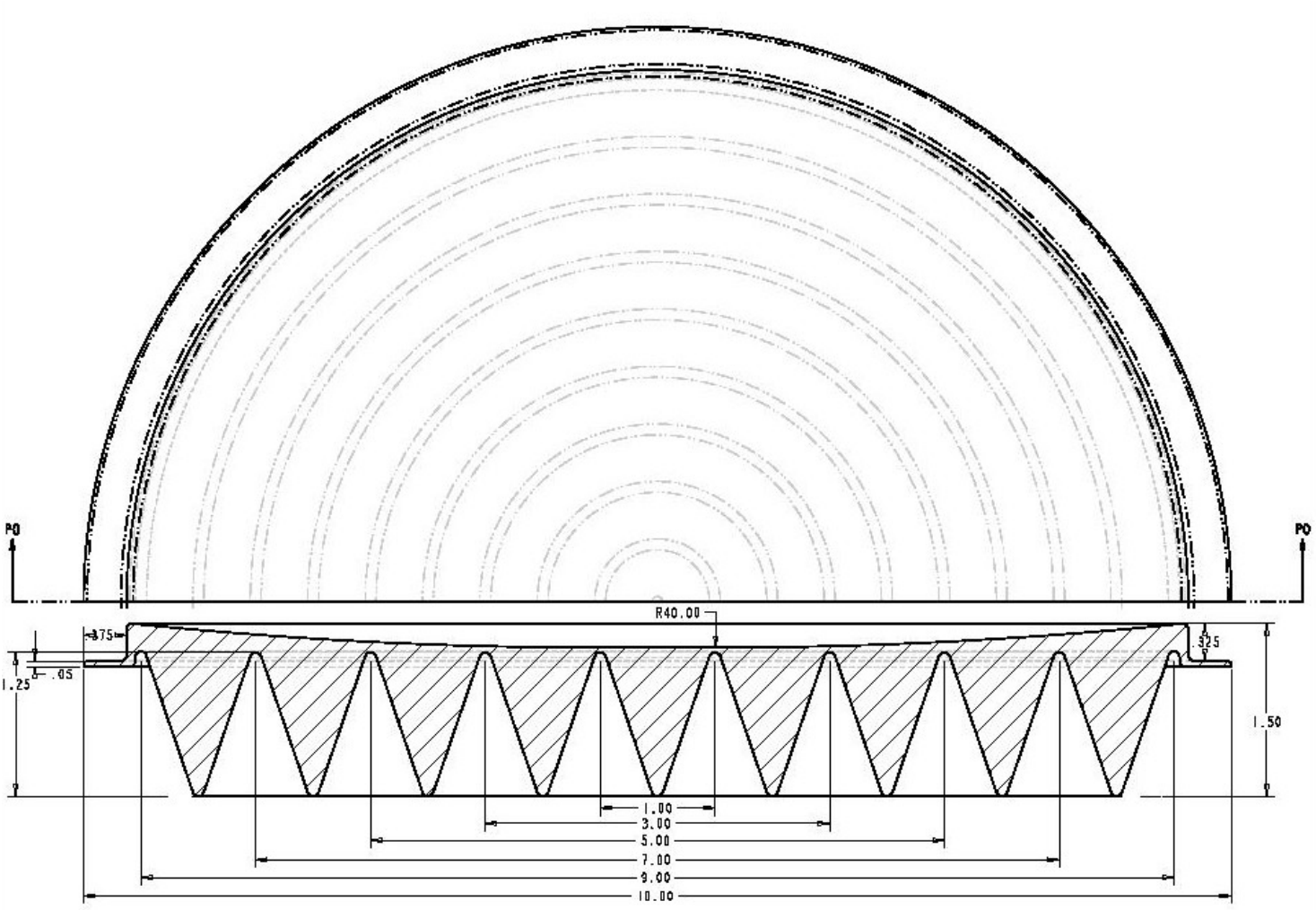

Figure 18: Module-top design (stainless steel material, units in inches)

As shown in Figure 18, both the concave indentation of the module top and the internal fins are preserved from the design proposed by Professor Wilson and his previous students. The predicted weight of steel was five pounds. The predicted volume of lithium nitrate is 1.9 l (4.1 kg).

C) Module construction

i) Material procurement & fabrication

(a) Module top

The selected design turned out to be too complex to fabricate at reasonable cost, utilizing equipment at the MIT central machine shop or at the MIT Laboratory for Manufacturing Productivity.

Figure 19: Manufactured module top

Instead, Laurel Brooke, an external machine shop in New Hampshire, manufactured the module tops. The top and bottom views of the product are shown above in Figure 19.

Type 304 stainless steel was ordered from Alliant Steel in New Hampshire. Aluminum was provided by Laurel Brooke.

(b) Module bottom

Stainless steel module bottoms (shown in Figure 20) were purchased from Hamilton Beach.

Figure 20: Module bottom

(c) Lithium nitrate

Lithium nitrate was initially purchased from Chemsavers at $50 per pound and then from Chemetall at a cost of $8.75 per pound.

ii) Assembly

(a) Components

The complete module consisted of a module bottom, enclosed lithium nitrate and a module top.

(b) Method choice

One challenge faced in assembling these components was maximizing the amount of lithium nitrate enclosed. This was consistent with the goal of minimizing occupied volume.

Lithium nitrate is supplied in granular form. In this condition, it has ½ the density of the crystalline solid and 2/5th the density of the liquid. To minimize occupied volume while leaving enough room for expansion upon liquefaction, the modules had to be filled with lithium nitrate in the liquid state.

The granular form was not used because, for the same weight of lithium nitrate, the volume occupied would be twice that of the liquid. The solid state was not used because it would require very high pressures to pack the lithium nitrate between the module's grooves.

(c) Method chosen

A sample of lithium nitrate weighing two pounds was placed into the module bottom. Both module bottom and lithium nitrate were then heated to 300 ^{0}C to melt and compact the entire sample. While the lithium nitrate was still molten, the module top (which was also heated) was placed over the bottom plate. The salt was allowed to solidify as it cooled to room temperature. The top and bottom plates were then joined and sealed.

iii)Joining and sealing

Once assembled the modules needed to be joined and sealed. The following methods were considered.

(a) Welding

Welding facilities are widely available, even in developing countries. Moreover, welding is relatively cheap and quick. Reasonable results can be produced by a novice.

One disadvantage of welding is the high temperature involved, since melting of the base metal is required. Stainless steel, for instance has a melting point of 1400 ^{0}C. The material safety data sheet for lithium nitrate states that exposure of lithium nitrate to high temperatures is an explosive hazard. However, this MSDS does not give a numeric value for what it considers high temperature. It does provide a value of 600^{0}C, as the temperature beyond which decomposition occurs. The combination of decomposition and/or explosion creates the possibility that high pressures will be developed in the module. Welding of containers subjected to high pressures is not recommended.

Furthermore, welding creates high-temperature gradients in the region close to the weld. Five minutes of heating at 600 ^{0}C produces chromium diffusion in steel, which will later lead to cracking. The chromium diffusion also reduces corrosion resistance.

(b) Soldering

Soldering involves the use of solder alloys which melt around 220 ^{0}C. Since the desired operating range for the module was as high as 300 ^{0}C, soldering was not an option.

(c) Brazing

Brazing would offer lower temperatures than welding. As shown in Table 12, silver-based brazing-alloys can be brazed at 760 ^{0}C. This is still higher than the upper temperature limit beyond which decomposition of lithium nitrate occurs. However, with cooling in the region of the brazed metal, temperatures in the lithium nitrate could be kept below 600 ^{0}C during brazing.

Table 12: Standard AWS brazing-alloy usage temperatures[9]

AWS 5.8 Spec's	°F	°C
BAg-1	1145-1400	618-760
BAg-1a	1175-1400	635-760
BAg-2	1295-1550	702-843
BAg-2a	1310-1550	710-843
BAg-3	1270-1500	688-816
BAg-4	1435-1650	779-899
BAg-5	1370-1550	743-843
BAg-6	1425-1600	774-871
BAg-7	1205-1400	652-760
BAg-8	1435-1650	779-899
BAg-8a	1435-1650	779-899
BAg-13	1575-1775	857-968
BAg-13a	1600-1800	871-982
BAg-18	1325-1550	718-843
BAg-19	1610-1800	877-982
BAg-20	1410-1600	766-871
BAg-21	1475-1650	802-899

(d) Mechanical fastening

This would afford ease of assembly and disassembly. However, the addition of bolts, nuts and a sealant (gasket or o-ring) would create an undesirable increase in the total weight of each module.

Shield metal arc welding (SMAW), also known as stick welding, was used. It is a commonly used process for containers with thick walls. The equipment is also easily accessible. However, the process affords less control to the welder, resulting in lower quality welds. Once briefed on the safety risks involved, and after being provided with the MSDS for lithium nitrate, the welders at the MIT central machine shop and ME Pappalardo laboratory were unwilling to perform the welding. To avoid exposing non-MIT welders to the aforementioned risks, Professor Wilson performed the welding himself.

D) Assembled module tests

The total weight of the assembled steel module was 8 lbs. The heating experiments consisted of heating the module from room temperature to a maximum temperature of 400 °C. The module was then removed and placed in an insulated storage container.

The following components were used.

i) Oven

Heat was supplied using a Thermolyne Furnatrol oven. The specifications list the maximum temperature as 1200 ^{0}C.

ii) Insulated storage container

Built by Jakob Hopping[22], this container contained a metal plate for supporting the heated modules. The plate was surrounded by fiberglass insulation. Elements of the design are shown below in Figure 21, Figure 22 and Figure 23.

Figure 21: Insulated storage container

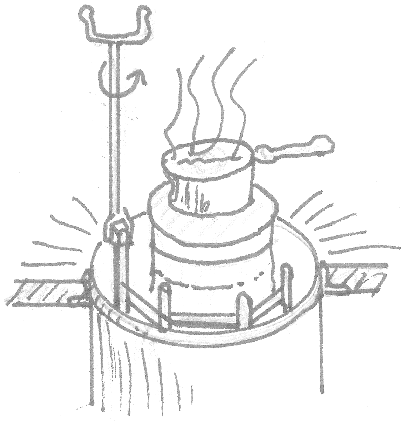

Figure 21 shows the manner in which the storage container is utilized during cooking. A pot is placed on top of the storage modules, which can be raised or lowered by rotating the handle.

Figure 22: Top and side views of the insulated storage container

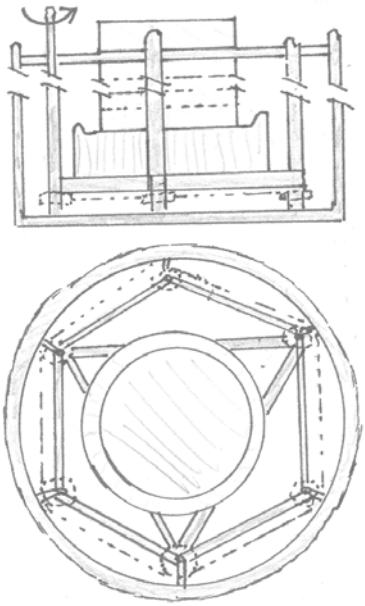

Figure 23: Metal drum used in construction of the insulated storage container:

iii)Temperature measurement

(a) Infrared thermometer

This thermometer utilized laser aiming, permitting temperatures to be monitored wirelessly. The thermometer had the following specifications:

Built in socket	accepted K-type or T- type thermocouples;
Measurement range	from -60 to 500 ^{0}C;
Probe ranges	from -83 to 1400 ^{0}C;
Ambient operating range	from 0 to 50 ^{0}C;
Accuracy	0.1 ^{0}C; and
Response time	1 second.

(b) Multimeter:

This multimeter was used to measure raw thermocouple voltages. It also had a socket for K-type thermocouples, which could be used to obtain temperature readings directly.

(c) K-type thermocouple.

Temperature was also measured using K-type wire thermocouples. Thermocouple calibration was performed using the above-mentioned multimeter temperature readings.

(d) Data logging equipment.

1.Hardware

Signals from the thermocouples were amplified and conditioned using a 4-channel WinDAQ module attached to a laptop via the serial port.

The WinDAQ module had the following specifications:

Four single-ended bipolar analog input channels;

10-bit precision;

+/- 10V ADC (analog to digital conversion) measurement range;

sampling rate up to 240 samples/second.

Amplification was provided by an Analog Devices AD595 thermocouple amplifier. This chip used an on-board ice point so there was no need to compensate for the ice point. The output was 10mV per ^{0}C.

2. Software

The laptop ran the WinDAQ software which displayed data in real-time and stored it for later use. The laptop was used in the Windows operating system enviroment.

E) Module re-design.

i) Design cycle two

Based on observations from the design implemented above, the following changes were made.

(a) Module material

The assembled module described above weighed eight pounds. That weight included two pounds of lithium nitrate. This was inconsistent with design specifications of 80 lbs for the maximum weight of the entire cooker. Two pounds of lithium nitrate in each module would necessitate 8 modules (weighing 64 lbs) in order to cook a meal for a family. To reduce this weight, aluminum was used in place of stainless steel for the module body.

(b) Coating

As explained earlier, some sources predicted undesirable (corrosive and explosive) reactions between aluminum and lithium nitrate. To prevent this, metal coatings were considered, to provide a barrier between the interior surface of the module top and the lithium nitrate. The module bottom was made of stainless steel, and so did not need to be coated.

Various finishes considered include:

1. anodization;
2. electropolishing;
3. galvanization; and
4. thermal sprays.

Because of cost, thermal sprayed coatings are only used extensively in aerospace applications They are used to a lesser extent, in commercial applications. However, they were chosen for this application because of their versatility with respect to material and thickness. Almost any material can be deposited using thermal sprays[23]. Stainless steel was sprayed on to the modules by Falmer Thermal Spray in Lynn, Massachusetts. The total cost for materials and services associated with the thermal spraying process was $200 per module.

(c) Shape design

Lastly, to improve manufacturability, the flange thickness Figure 18 was increased from 0.05 inches to 0.375 inches. Instead of one, five modules were manufactured. The same (commercial, off-the-shelf) module bottom was used as in the first design cycle.

(d) Joining

At temperatures above melting, the module tested above consistently leaked small amounts of lithium nitrate. Because of this leakage, it was necessary to change, or at least improve, the mechanism of joining the module top to the bottom. Instead of brazing, the following joining methods were considered.

1. Mechanical fasteners

Mechanical fasteners would have the advantage of being easy to disassemble and reassemble. In turn, this would improve the ease of manufacture and maintenance, especially since most target users are in countries rapidly undergoing technological development. Thus, bolts were chosen to fulfill this requirement.

The modules were bolted along the flanges, using 10 evenly spaced 3/8-bolts and matching nuts.

2. Sealants

With the use of mechanical fasteners, sealants would be necessary for the complete prevention of liquid, or gaseous, leakage of lithium nitrate. The following sealants were considered:

a O-rings

O-rings are commonly made of rubber. Thus, they would offer the most pliancy and flexibility. However, little was known about the interaction between rubber and lithium nitrate. The only guidance available was from the material and safety data sheet (MSDS), which stated that lithium nitrate was incompatible with organic materials.

In addition, o-rings would require grooves on the module flanges. This would add complexity to the manufacturing of the modules.

b Ceramic gaskets.

Ceramic gaskets would offer the advantage of simplicity, since grooves on the flanges were not required. Another advantage stems from the fact that ceramics are relatively inert.

A ceramic (alumina) gasket tape was available from Richards Sensors at low cost. Its specifications indicate that it was thermally stable up to 650 ^{0}C. This gasket tape was tried in one heating experiment. The material disintegrated upon interaction with lithium nitrate. Consequently, ceramic gaskets were removed from further consideration.

c Metal gaskets

Of all sealant materials considered, the easiest outcome to predict was associated with the use of metals as gaskets. This is because more was known about the interaction of lithium nitrate with metals, than with other materials. In addition, previous tests conducted as part of this study could shed light on the gasket metals being considered. The gasket shown below was available from MDC vacuum products in Hayward, California. None of the dimensions available matched the flange of the module being used for the test. Hence, the modules would have to be redesigned to be able to take advantage of off-the-shelf gaskets.

Figure 24: MDC Copper gasket

d Silicone sealants

Most silicone sealants were not suitable for use at the high temperatures (300 ^{0}C) involved in these tests. The highest rated material found in this category was Red Polyseamseal. The manufacturer's specifications were as follows[24]:

1. permanently flexible from -85 to 500 ^{0}C;
2. short-term exposure to 600 ^{0}C ; and
3. seals and encapsulates heating elements in engines and most high-temperature sealing applications.

After analyzing the four sealing methods described above, Red Polyseamseal (a silicone sealant) was chosen because of the ease with which the modules could be assembled and disassembled, as well as the ease of procurement.

(e) Assembly

The assembly was modified by preheating lithium nitrate and the module bottom in a kitchen oven, instead of using a hot plate.

ii) Redesigned module test

Heating experiments were conducted using multiple modules, instead of one. The experimental setup was the same as in Chapter 3, paragraph D.

Chapter 4) Results and discussion

Six modules were fabricated, assembled, and tested in conjunction with the insulated storage container. This section presents the observations made during testing.

A) Health risks

In accordance with the MSDS, it was observed that lithium nitrate severely irritates the skin, eyes and respiratory tract. Therefore, gloves and a mask were worn during testing in order to minimize health risks.

B) Chemical and physical properties

The literature search had yielded unacceptably vague and sometimes conflicting predictions about lithium nitrate's compatibility with metals. Similarly, predictions about lithium nitrate's stability at high temperatures were inconclusive.

i) Test 1: stainless steel cup and mild steel cap

(a) Reactivity

1. Stainless steel
   No corrosion was observed on the steel cup. This suggests that there was no significant reaction between lithium nitrate and stainless steel.

2. Mild steel
   Some oxidation was observed on the mild steel cap. This could be from reacting with the lithium nitrate or from ambient air. In either case, the observed oxidation discouraged further consideration of mild steel.

(b) Compatibility

Contrary to theoretical predictions, no explosion was observed, with the stainless steel, mild steel or even with aluminum foil. All three metals were exposed to lithium nitrate at temperatures as high as 300 ^{0}C. Neither brazing nor welding of steel was accompanied by explosions.

(c) Physical properties

Lithium nitrate appears to vaporize at temperatures as low as 300 ^{0}C. As described in the Methods chapter, the lithium nitrate was enclosed in a steel cup and covered with a steel cap. Both were tapered, to form a liquid-tight seal. At the end of three weeks of repeated heating and cooling (504 cycles), it was observed that 50% of the lithium nitrate had escaped from the steel cup enclosure. This lithium nitrate was deposited on the walls of the surrounding aluminum foil that was being used as a heat shield. Most of the lithium nitrate deposits were found on areas of the foil above the steel enclosure. If the escaping lithium nitrate was in the liquid form, it would simply have dropped to the areas adjoining the steel enclosure. The only reasonable explanation for finding lithium nitrate deposits at heights above the enclosure, is that the lithium nitrate vaporized and condensed upon coming into contact with the aluminum foil barrier at lower temperatures (perhaps during the cooling phase of the heating-cooling cycle).

This leads to the conclusion that lithium nitrate must have come into contact with the aluminum foil at temperatures above its melting point. Since no evidence of corrosion or explosions were observed, there seems to be a very strong possibility that aluminum and lithium nitrate are compatible at temperatures below 300 ^{0}C.

ii) Test 2: mild steel flat pouch

Jakob Hopping conducted this test. He experienced difficulty heating the entire pouch to melting. Possible explanations for this observation are detailed in the next section (thermal energy storage results). Even though the material at the edges could not be melted, he was able to melt the lithium nitrate at the center of the pouch. No corrosion or explosions were observed.

This leads to the conclusion that mild steel is compatible with lithium nitrate. However, mild steel oxidizes in air. Hence, unless it is coated with another material, its durability - simply from exposure to atmospheric conditions - would be unsatisfactory for the desired life cycle (more than a year) of the WSC.

C) Thermal property observations

As shown in Table 6, the critical thermal properties of solid lithium nitrate are listed below.

Heat of fusion	367 kJ/kg
Specific-heat capacity	385 J/kgK
Conductivity	0.5 W/mK

Equivalent tiquid state properties were not found in the literature.

Lithium nitrate turned out to be a very difficult material to work with during assembly. In both tests two and three (above), it proved quite challenging to melt less than three pounds of the material in a module using an 1100 W heater. The center areas receiving the most heat, melted within 30 minutes. However, the areas beyond a diameter of four inches would not melt even after an hour.

Three possible explanations arise.

i) High surface area to volume ratio

The pouch and the module were designed to have a very large surface area in comparison with their total volume. The goal was to facilitate uniform distribution of heat within the module via conduction.

The surface area to volume ratios of the module and pouch are 100 times greater that of a cube. This has a significant impact on conducting heating tests with the module and pouch. During charging, mechanisms have to be set up to prevent the high rate of heat loss which would ordinarily result from the large surface area.

ii) Low conductivity of lithium nitrate

The thermal conductivity of lithium nitrate is low (0.5 W/mK). This is one-quarter the thermal conductivity of ice.

According to the Equation 2, the rate of conduction of thermal energy from the center to the edges is directly proportional to the thermal conductivity of lithium nitrate. Since low thermal conductivity leads to poor conduction, it is possible for the material on the edges to remain unmolten while the material in the center of the pouch/module melts.

iii)High latent-heat capacity

A third reason for the observed behavior is the relatively high latent heat of melting (367 kJ/kg) for solid lithium nitrate. The amount of heat required to melt a given mass of lithium nitrate is proportional to its latent-heat capacity. The time taken to melt the lithium nitrate is therefore directly proportional to the latent-heat capacity. Since lithium nitrate was chosen for its high latent-heat capacity, it can be expected that the time required for melting would also be high.

Expectations based on the last two factors (low thermal conductivity and high latent heat) are contradicted by the observations that the molten lithium nitrate cooled very rapidly. There was little time (minutes) between melting and re-solidification. The module top had to be in place within that time interval. Otherwise the lithium nitrate would re-solidify, rendering it impossible to wedge the fins in the lithium nitrate as the design called for (in order to minimize occupied volume). In addition, if the emplaced module top was at room temperature, the lithium nitrate would re-solidify upon contact with the module top (rendering it impossible to move the module top to the correct mating position). Hence, the module top was pre-heated to the same temperature as the melting point of lithium nitrate (258 ^{0}C).

Such manipulation of the module components, at temperatures as high as 258 ^{0}C, will definitely pose an issue during manufacturing. There are significant risks involved that would invite further re-examination of the assembly process.

D) Thermal energy storage results

i) Test 3: single steel module

Figure 25 shows the variation of temperature over time for a single module made up of stainless steel and filled with two pounds of lithium nitrate.

The module was heated to 400 ^{0}C and then placed in an insulated container. As shown on the chart, the temperature dropped from 400 ^{0}C to 200 ^{0}C in three hours. The highest rate of temperature drop occurred in the first 30 minutes. During that time, the freezing point was reached. The rate of cooling slowed down as time progressed.

Figure 25: Temperature versus time in a stainless steel module

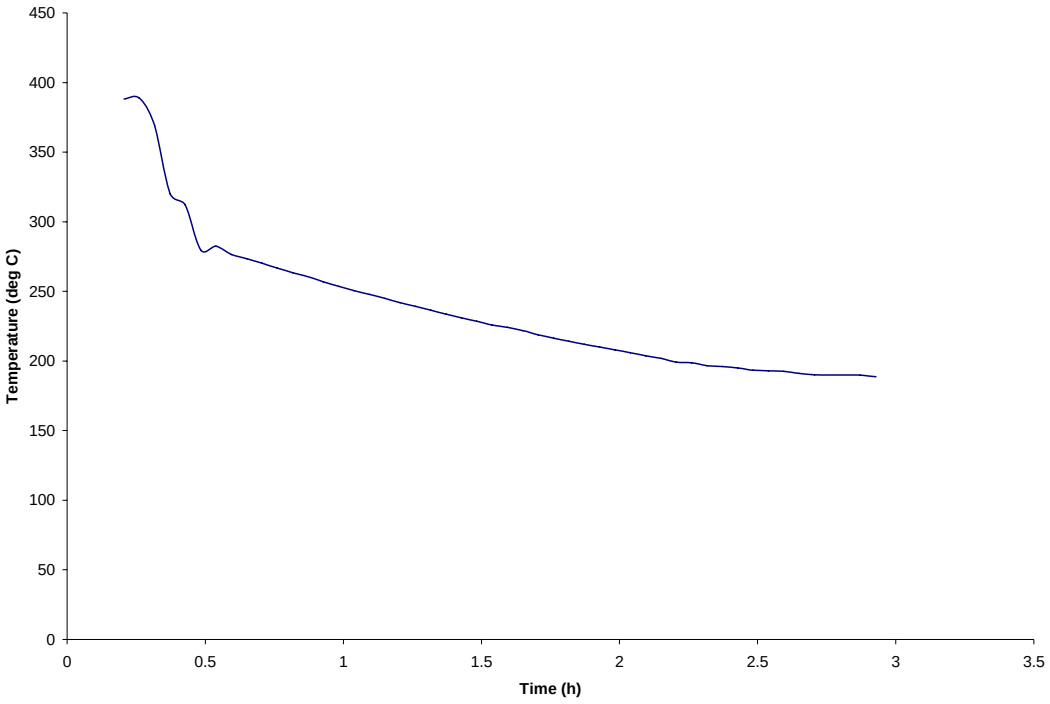

This is not the result expected. There should have been three distinct regimes, as shown in Figure 26.

Figure 26: Theoretical predictions for temperature versus time in a pure substance cooled at constant pressure

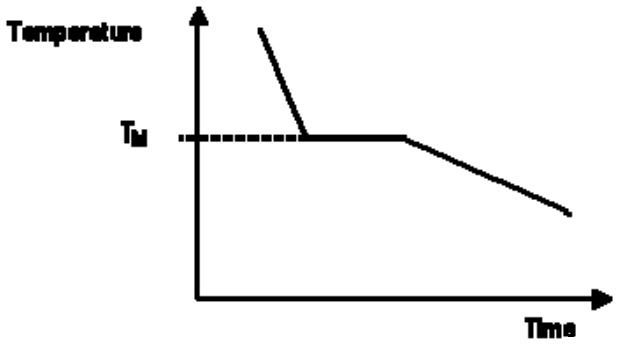

(a) Temperature drop above the melting point

Given that most sources record a melting point of 258 ^{0}C for lithium nitrate, it would be expected that the temperature would initially drop at a relatively constant rate, from above melting to the melting point. The average slope during this initial temperature drop would be expected to be negative.

Since the rate of heat loss is proportional to the temperature difference, this initial temperature drop should be the fastest. This is in accordance with observations.

(b) Temperatures at the melting point

It would then be expected that the temperature remains approximately constant, long enough to be detected on the temperature-time chart, until all the lithium nitrate solidifies. No such slope change was observed in this test. The slope of the temperature-time chart, within the interval five degrees above and below the melting point, is approximately the same as the rest of the curve. This discrepancy raises the question of how effective the modules would be for cooking at constant temperature or for storing energy as latent heat.

(c) Temperature drop below the melting point

Once solidification is complete, the temperature drop would be expected to continue until room temperature is reached. The observed values for the temperature drop after melting, are shown below in Figure 27. As expected from Equation 4, approaching room temperature causes the rate of temperature drop to decrease exponentially.

Figure 27: Temperature versus time of lithium nitrate in a stainless steel module (after solidification)

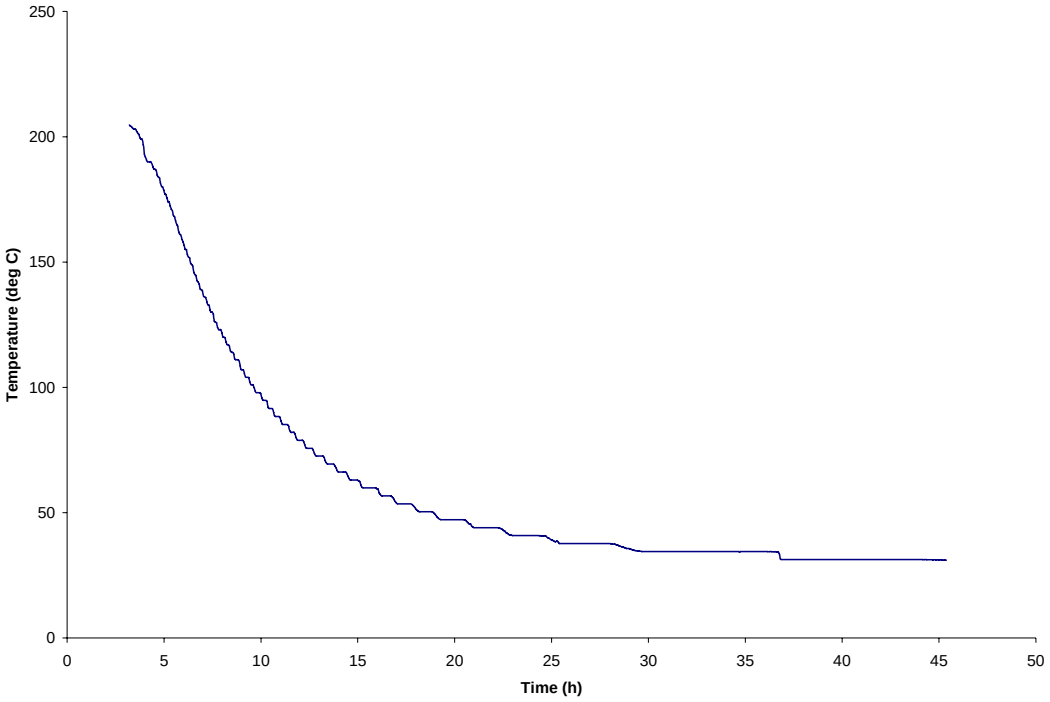

Figure 28 shows results from a similar test, but with a different kind of insulation. Instead of fiberglass, sawdust was used. The temperature drop from 200 ^{0}C to 100 ^{0}C is much faster than is shown in Figure 25. This can be attributed to the increase in thermal conductivity of the loosely packed sawdust, as compared with fiberglass.

Figure 28 also provides information on the rate of heat conduction within the module. Temperature versus time measurements were collected from two locations on the module. The first location was dead center on the bottom of the module. The second location was on the top edge. As shown on the chart, throughout the period of data collection (three hours), a temperature difference of 15 ^{0}C was observed between the two thermocouple locations.

Figure 28: Temperature difference across a single steel module in sawdust insulation

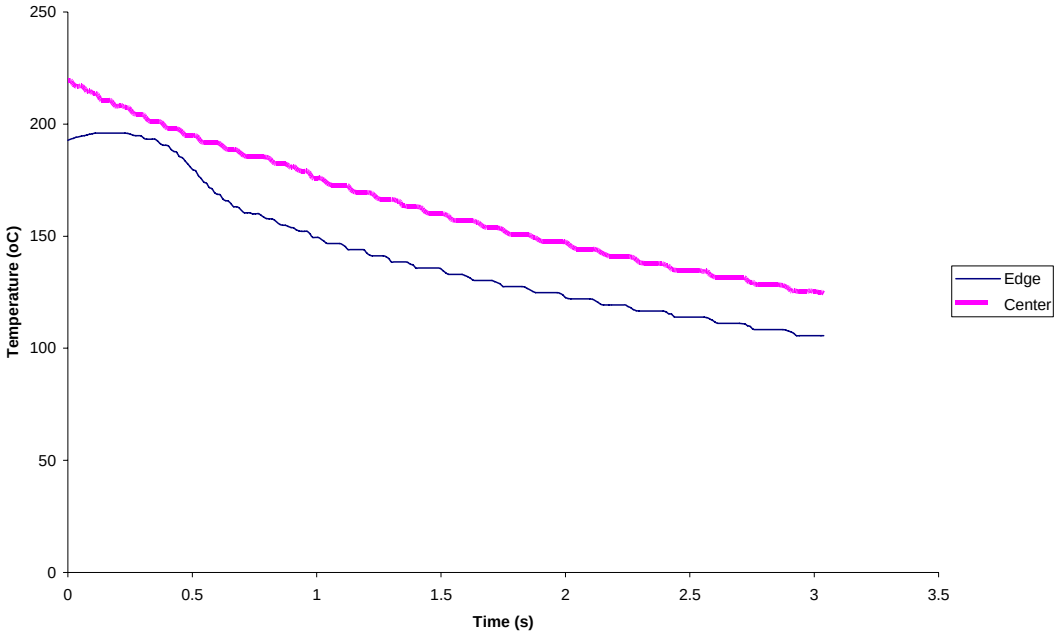

This is in conflict with the known value of thermal conductivity for stainless steel, which is 16.3 W/m-K. A temperature difference of 15 ^{0}C across a module 10 inches in diameter and one inch thick would not be expected.

ii) Test 4: two aluminum modules

In this test, one module was heated to 300 ^{0}C and placed in the insulated storage container. Three hours later, another module heated to 300 ^{0}C was added to the insulated storage container. Subsequently, the temperatures of both modules were recorded.

Figure 29 shows that the new module's temperature started at 300 ^{0}C, dropped to 240 ^{0}C and remained constant for approximately six hours. Compared with test three (single module), this behavior is more consistent with expectations for temperature variation during storage.

(a) Temperature drop above the melting point

The initial rate of temperature drop is the highest observed throughout the test. This is in accordance with Equation 2, which predicts that heat loss would be proportional to the temperature difference between the module and its surroundings.

Figure 29: Temperature versus time for two modules in a pre-heated storage container

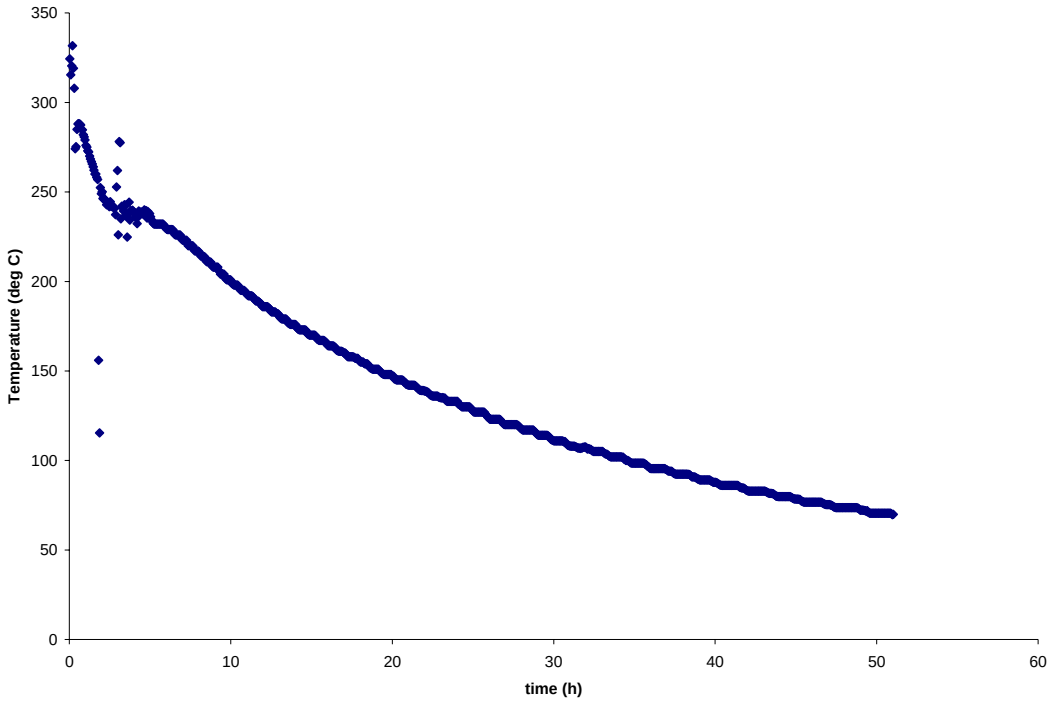

(b) Temperatures at the melting point

It was observed that the temperature remained approximately constant long enough to be detected on the temperature-time chart (in this case four hours), until the entire lithium nitrate solidified. This is in accordance with predictions for the usefulness of the modules during cooking. This chart confirms the feasibility of cooking food at constant temperature of 240 ^{0}C for four hours.

(c) Temperature drop below the melting point

At that point, the temperature drop would be expected to continue until room temperature is reached. The observed values for temperature drop to room temperature are shown above in Figure 29. As expected, approaching room temperature causes the rate of temperature drop to decrease exponentially. The temperature stayed above 125 ^{0}C for 25 hours. It remained above 50 ^{0}C for more than 50 hours.

iii)Test 5: three aluminum modules

In this test, two modules heated to 300 ^{0}C were placed in the insulated storage container. Three hours later, another module heated to 300 ^{0}C was added to the insulated storage container. Subsequently, both the temperatures of the initial modules and that of the new module were recorded.

Figure 30 shows that the last module's temperature started at 270 ^{0}C and remained constant at 250 ^{0}C. It did not drop to 240 ^{0}C until after six hours. Compared with test four (two modules), this behavior is even more consistent with expectations for temperature variation during storage.

Figure 30: Temperature versus time for three modules in a pre-heated storage container

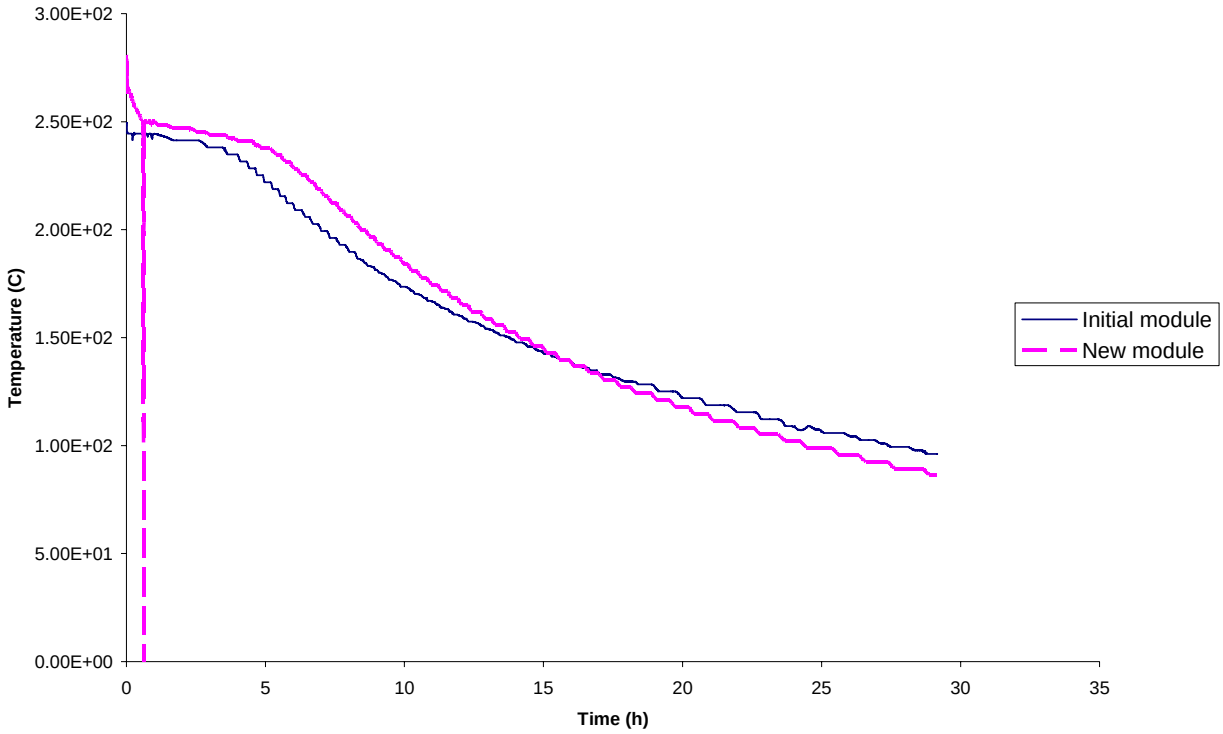

(a) Temperature drop above the melting point
As in the two previous tests, the initial rate of temperature drop before solidification was higher than after solidification. This is consistent with expectations.

(b) Temperatures at the melting point
In comparison with test four (two modules), the period of solidification is longer – six hours. This is to be expected since more modules (three) were used in this test.

(c) Temperature drop below the melting point
As expected, approaching room temperature caused the rate of temperature drop to decrease exponentially. The temperature remained above 125 ^{0}C for 30 hours.

E) Key system parameters

Utilizing the observations recorded in the preceding paragraphs of this section, it is now possible to evaluate some of the system parameters identified as key, at the beginning of this project.

i) Heat-absorption rate during charging

The concentrator and absorber were not incorporated into this project, owing to time constraints.

ii) Heat-loss rate during storage

The rate of heat loss depends on three factors.

(a) Heat-storage phase

Heat loss was calculated by using the rate of temperature drop in the modules, as well as the mass of lithium nitrate in the modules. The mass of the module container was ignored.

Table 13: Heat-loss rate as a function of heat-storage phase

mass of lithium nitrate (kg)	1.4	
latent heat phase		
time required for solidification (h)	latent heat of fusion (J/kg)	heat loss rate (W)
6	367000	23.79
sensible heat phase		
temperature drop rate (^{0}C/h)	specific heat capacity(J/kgK)	heat loss rate (W)
5	385	0.75

As shown in Table 13, the rate of heat-energy loss during melting was 30 times that observed upon re-solidification. This ratio is far higher than would be expected, since the insulation is the same. The only possible reasons for the difference (between latent- and sensible- heat-storage loss) are listed below.

1. Higher thermal conductivity

   The liquid lithium nitrate in the molten state had a higher thermal conductivity than in the solid state.

2. Heat losses through convection

   In the liquid state, lithium nitrate could lose heat through convection as the salt moves inside the module.

Table 14: Predicted heat-loss rate as a function of temperature difference.

Temperature difference (K)	Heat loss rate (W)
20	8.81
40	13.44
60	18.11
80	22.75
100	27.42
120	32.08
140	36.72
160	41.39
180	46.03
200	50.69
220	55.36
240	60.00
260	64.67
280	69.33
300	73.97
320	73.97
340	83.28
360	87.94

3. Higher temperature differences

In the molten state, temperatures were higher than in the solid state. The resulting temperature differences (between the module and its surroundings) led to higher rates of thermal conduction and thermal energy loss in the molten state. This agrees with predictions, as shown in Table 14, that the heat-loss rate increases at higher temperatures.

Neither factor accounts for the large discrepancy between the latent-energy heat-loss rate on one hand, and the sensible-energy heat-loss rate on the other.

(b) Number of modules stored

For the module test results shown in Table 15, additional modules were placed in the storage container at different times, approximately three hours apart.

Table 15: Heat-loss rate for varying numbers of modules

mass of lithium nitrate per module (kg) 1.4 latent heat of fusion (J/kg) 367000		
Number of modules	time required for solidification (h)	total heat loss rate (W)
1	0.5	285.44
2	4	35.68
3	6	23.79

This was done to simulate the manner in which the modules would be removed from charging, at intervals of approximately one hour.

The number of modules stored is a very important variable when it comes to the rate of heat loss from the system. Table 15 shows that the first module lost its thermal energy ten times faster than the third module.

This is to be expected, since the rate of heat lost through thermal conduction is directly proportional to the temperature difference (between the module and its surroundings). The temperature difference was lowest in the case of three modules.

(c) Insulating material

Table 16: Predicted heat loss as a function of insulation thickness.

Insulation thickness (in)	Heat loss (W)
7	87.75
8	84.69
9	82.50
10	80.97
11	79.86
12	79.14
13	78.67
14	78.31
15	33.33
16	78.36
17	78.50
18	78.75
19	79.08
20	79.47
21	79.92
22	80.42
23	80.94
24	81.53

Table 16 shows the results of predictions made by a previous student for the heat-loss rate as the insulation thickness is varied. Table 17 shows that the nature of the insulating material has a significant effect on the heat-loss rate. In this test, the insulating capacity of the sawdust was significantly reduced because it was loosely packed.

Table 17: Heat-loss rate for different insulating materials

Mass of lithium nitrate (kg)	1.4		
Specific heat capacity(J/kgK)	385		
Insulation material	Thermal conductivity (W/mK)	Temperature drop rate (deg/h)	heat loss rate (W)
Fiberglass	0.04	12.5	1.87
Sawdust	0.042	25	3.74

iii)Heat-transfer rate during cooking

No tests were conducted to determine the rate and efficiency of thermal energy transfer from thermal battery to pot during cooking. This would be the next step recommended for future tests.

iv) Useful heat

Even though the results for temperature versus time were sometimes surprising, observations on the proportion of heat stored that can be transferred to a cooking pot are not. Table 15 shows that heat is lost from each module at a rate of 23W, during solidification. If averaged throughout cooling, the fraction of useful heat lost is 3% per hour. Figure 30 shows that the temperature remains relatively static at above 258 ^{0}C for more than six hours. Furthermore, once the temperature drops below the phase-change point, it remains higher than 100^{0}C for more than 25 hours. It is therefore to be expected that the WSC would be able to supply the 13MJ needed to cook a three-pound meal many hours (at least six) after charging is complete.

v) Maximum system temperature

As shown in the above graphs, if the system is leak-proof, it can attain temperatures as high as 400 ^{0}C without any negative effects. The Red Polyseamseal sealant was the only component degraded during operation at this temperature.

This provides some answers to the questions raised by the vague and sometimes conflicting data in the literature about thermal decomposition and stability of lithium nitrate at “high” temperature. It suggests that 400 ^{0}C is not high enough to cause any of the predicted explosive hazards.

Since measured values of the vapor pressure as a function of temperature are not available, tests should be conducted to ascertain the vapor pressure developed during heating.

Chapter 5) Conclusion and Recommendations

After completing the analysis, design and testing of the heat-storage system, the following suggestions are offered to assist with future work on this project.

A) Design

i) Materials selection

(a) Heat-storage-material

Lithium nitrate, the heat-storage material, has been shown to meet the stated requirements of storing heat at a constant temperature of 258 ^{0}C for up to six hours. Furthermore, this heat-storage material stores heat at temperatures above the boiling point of water, for up to 25 hours. Thus, it is expected that a meal for up to six people can still be prepared six hours after charging.

(b) Module-body material

1. Weight

The choice of material for the module body has a significant impact on the weight of the module and of the entire system. The assembled steel modules weighed eight pounds. The assembled aluminum module weighed four pounds. If users are to be expected to manipulate these modules between the charging and cooking phases, the steel modules are too heavy. The weight of the aluminum modules is more acceptable.

2. Availability

Both aluminum and steel are widely available in virtually every country. To reduce costs, recycled metals could be used

3. Compatibility

The observation that lithium nitrate may be compatible with aluminum at temperatures below 300 ^{0}C deserves further examination. Since the density of aluminum is one-third that of steel, this would lead to a proportional reduction of the total weight of the WSC. This would also eliminate the need for thermal spraying, which costs more than $200 per module. Even at commercial production rates, because of cost, spraying would not have been a feasible option.

In view of the above observations, the recommended module-material is aluminum. It has the lowest cost and the lowest density. It also is the easiest to manufacture.

ii) Module construction

(a) Fabrication

The current weight (four pounds) of the aluminum modules is acceptable. However, it can be reduced by using (rolled or drawn) aluminum sheets, instead of machined aluminum. This would possibly cut the weight, and cost, by up to one-third of the current values.

The current module shape (with internal fins) requires advanced manufacturing equipment readily available, only in industrialized countries. Once a prototype is available, casting can be used for production runs.

(b) Assembly

The current assembly process requires exposure of the assembler to very high temperatures of 258 ^{0}C. This might be addressed by automating the process, if demand rises to volumes high enough to sustain the additional cost.

(c) Joining and sealing

Mechanical fasteners (in conjunction with sealants) are easy to assemble and disassemble. However, welding and brazing have the advantage of being much more accessible in most countries of interest.

iii)Module-shape design

As mentioned earlier, the internal fins would be difficult to manufacture in non-industrialized countries. A simpler shape, such as a thin flat disk, would significantly widen availability of manufacturing equipment.

The current design calls for users handling modules at high temperatures (258 ^{0}C). Professor Wilson[25] has proposed adding handles made of a material with very low thermal conductivity (such as foam or ceramic glass). These handles would maintain temperatures that a user could touch without being harmed.

The temperatures in question involve a high level of risk as far as user safety is concerned. From discussions with Professor Wilson[24], it appears that it will be worthwhile to eliminate the possibility of users being exposed to the modules at such high temperatures. The system could be designed so that the absorbed thermal energy is conducted through metal pipes or rods to the insulated modules during charging, and released from the modules in the same position during cooking. The user would not have to move the modules in between charging and cooking, when the temperatures are highest.

B) Performance

Tested components of the Wilson solar cooker display the potential for performing satisfactorily, storing heat at a constant temperature of 258 ^{0}C for up to six hours.

The quality of insulation alters the heat-storage-capacity period of the system by more than one order of magnitude. For instance, changing from fiberglass to sawdust cuts the storage time by half.

Referring to Table 18, fiberglass provides adequate insulation. However, it poses health risks, because it inflames the respiratory tract. Styrofoam melts at low temperatures. Aerogel may not be available in non-industrializing countries. Concrete or brick are commonly available and are recommended for further use as the insulating material.

Continuously maintaining the storage container at temperatures above room temperature would also greatly improve the heat-storage capacity of the system

The next set of tests should be conducted with heating loads (food to be cooked) added to the system.

Table 18: Thermal conductivity of common materials

Material	Thermal conductivity (W/m K)*
Silver	406
Aluminum	205
Glass,ordinary	0.8
Concrete	0.8
Water at 20 C	0.56
Asbestos	0.16
Brick,insulating	0.15
Wood	0.13
Snow (dry)	0.12
Saw dust	0.042
Fiberglass	0.04
Cork board	0.04
Wool felt	0.04
Rock wool	0.04
Air at 0 C	0.024
Aerogel	0.016
Styrofoam	0.01

C) Deferred features

Some of the features deferred at the beginning of the project are listed below.

i) Salt-state indicator

ii) Operator control of stovetop heat-transfer rate during cooking.

iii)Automatic tracking of the sun's apparent movement.

The following components were deferred for later research as the project progressed.

iv) Radiant energy collection

v) Thermal energy absorption

vi) Cooking

As mentioned in the background section, commercial parabolic solar cookers do attain relatively high temperatures. In the mid-temperature range, a power output of 500 watts can easily be attained. Since the Clear Dome solar cooker's temperatures are as high as 1371 ^{0}C, attaining a desirable heat-absorption rate becomes merely a question of finding an appropriate absorber and developing a tracking scheme. In comparison with development of the heat-storage mechanism, it is to be expected that development of the concentration and absorption scheme will be much more straightforward.

REFERENCES

[1] Bowman, T. *Understanding Solar Cookers*. Arlington: Volunteers in Technical Assistance; 1985.

[2] Wyman, C. A review of collector and energy storage technology for intermediate temperature applications. *Solar Energy*. 1980; 24: 517-540.

[3] Solar Cookers International. The Solar Cooking Archive. Available at http://www.solarcooking.org. Accessed 9 August 2004.

[4] K&K Associates. Thermal finishes. 2005. Available at http://www.tak2000.com/data/finish.htm. Accessed 27 May 2006.

[5] Matteo, BC. *Stored-heat solar cooker*. (SB Thesis, Massachusetts Institute of Technology; 1995).

[6] Radabaugh, JM. *Heaven's flame* Ashland: Home Power; 1998.

[7] *Solar Cooker Construction Manual.* Arlington: Volunteers in Technical Assistance; 1967.

[8] Buddhi D, Sharma SD, Sharma A. Thermal performance evaluation of a latent heat storage unit for late evening cooking in a solar cooker having three reflectors. *Energy Conversion and Management.* 2003; 44: 809-817.

[9] Sharma SD, Iwata T, Kitano H. Experimental results of evacuated tube solar collector for use in solar cooking with latent heat storage. *Proceedings of the EM4 Indoor Workshop IEA ECES IA Annex, 2004*; Indore, India. Available at http://www.fskab.com/Annex17/Workshops/EM4%2520Indore%25202003-03-21--24/Presentations/SDSharma%2520PAPER.pdf. Accessed 30 April 2006.

[10] Murty, VV. Thermal performance of a solar cooker having phase-change material as transparent insulation. *Proceedings of the EM4 Indoor Workshop IEA ECES IA Annex, 2004*; Indore, India. Available at http://www.fskab.com/Annex17/Workshops/EM4%20Indore%202003-03-21--24/Presentations/VVS_murty.pdf. Accessed 30 April 2005.

[11] Wilson, DG. *The Wilson Thermal-Storage Solar Cooker.* (Concept Memo and Pre-proposal, Massachusetts Institute of Technology; 1997)

[12] Mkandawire, C. *Designed and Modeled Solar Cooker.* (SB Thesis, Massachusetts Institute of Technology; 1994).

[13] Mallinkrodt Chemicals. Material safety data sheet L6958. Available at http://www.jtbaker.com/msds/englishhtml/l6958.htm. Accessed May 30, 2006.

[14] Automation creations. *Material property data*. Available at http://www.matweb.com. Accessed April 25, 2006.

[15] Palmer, J. Brazing and welding 304L stainless steel. *Brewing techniques* [serial online] 1994; 2:6. Available at: http://www.brewingtechniques.com/library/backissues/issue2.6/palmer.html. Accessed April 25, 2006.

[16] *Stainless steel- fabrication*. Available at http://www.azom.com/details.asp?ArticleID=1178. Accessed 27 Apr 2006.

[17] Lovering, DG (Ed). *Molten salt technology.* New York: Plenum Press; 1992

[18] Phone conversation, August 2004 with Dr. Robert Bradshaw

[19] Phone conversation, January 2005 with Dr. David H. Kerridge

[20] Hopping, JA. *Solar Cooker Progress/Data.* (UROP rogress report, Massachusetts Institute of Technology; 2005).

[21] Washburn, EW. *Knovel International Critical Tables of Numerical Data, Physics, Chemistry and Technology* (1st Electronic Edition). 1926 - 1930; 2003: pp. 24). Online version available at:http://www.knovel.com/knovel2/Toc.jsp?BookID=735&VerticalID=0. Accessed April 25, 2006

[22] Hopping, JA. *Development of a solar cooker* (UROP Report, Massachusetts Institute of Technology; 2005).

[23] Thermal Sprayed Industrial Coating. *Engineers Edge.* Available at http://www.engineersedge.com/finishing/thermal_spray_coating.htm. Accessed May 13, 2006

[24] Barr, TF. *Red high-temp silicone sealant.* Mentor: OSI Sealants; 1999

[25] Email correspondence with Professor Wilson, May 15, 2006